

## 5. RESEARCH ACTIVITIES

### 1. NUCLEAR PHYSICS

S.K. Datta and R.K. Bhowmik

The major achievement of the Nuclear Physics group during the period 2002-2003 has been setting up of the Indian National Gamma Array (INGA) at Nuclear Science Centre. It was decided to set up this facility in the HIRA beam line to perform recoil-gated  $\gamma$ -spectroscopy for the study of weakly populated channels. The Clover detectors and the associated electronics were pooled from IUC-DAEF, SINP, TIFR, BARC, VECC and NSC.

A mechanical structure to mount up to eight Clover detectors around the target location for HIRA was fabricated which could also accommodate four neutron detectors for neutron-gated spectroscopy. The Charged Particle Array from TIFR was installed in the beam line for additional channel selection.

A high speed multi-crate data acquisition system *CANDLE* has been developed for the collection of  $\gamma$ - $\gamma$ ,  $\gamma$ - $\gamma$ -recoil and  $\gamma$ - $\gamma$ - $n$  coincidence data. The number of  $p$  &  $\alpha$  particles produced in the reaction were also recorded event by event. An indigenously developed computer-controlled system has been used for automatically filling the clover detectors with liquid nitrogen at periodic intervals. Dedicated electronics modules for processing all the signals from a Clover detector have been developed and tested with the INGA array.

Preliminary tests with the reaction  $^{28}\text{Si} + ^{58}\text{Ni}$  at 95-115 MeV indicated that the various recoil products ( $A = 80 - 84$ ) from the compound nucleus  $^{86}\text{Mo}$  could be identified in the recoil separator and the recoil-gated  $\gamma$ -spectra were significantly cleaner than the un-gated  $\gamma$ -spectra with little contamination from the neighbouring channels.

During the period Nov, 2002 — March, 2003 the following experiments have been conducted using the INGA array :

2. Investigation of the shears mechanism in  $^{112}\text{Sb}$
3. In-beam  $\gamma$ -spectroscopy of  $^{125,126}\text{Cs}$
4. Spectroscopy of light neutron rich nuclei ( $^{35}\text{P}$ ,  $^{36}\text{S}$ ,  $^{34}\text{Si}$ ..) using the transfer in near barrier & sub-barrier heavy ion reactions
5. Study of high spin states in  $^{138}\text{Ce}$
6. Search for magnetic rotation in  $^{138}\text{Nd}$
7. Study of n-p interaction in  $N = Z$  Nuclei in mass 80 region
8. Search for Chiral bands in  $^{109}\text{Ag}$
9. Spectroscopy of Ar and K isotopes in  $A=40$  region
10. Study of superdeformed bands in sd-shell nuclei
11. High spin spectroscopy of  $^{52}\text{Cr}$

12. Lifetime measurements for the magnetic rotation bands in  $^{79}\text{Rb}$
13. Excitation of highly deformed bands in  $^{44}\text{Ti}$  following fusion-fission decay of  $^{52}\text{Fe}$ .

Data analysis for these experiments are in progress. Two more experiments are planned using the INGA facility during the month of April, 2003.

The RIB facility at NSC has been extensively used during April, 2002 to June, 2002 for the study of nuclear scattering/reactions with  $^7\text{Be}$  projectiles. The astrophysical  $S_{17}$  factor from the reaction  $d(^7\text{Be}, ^8\text{B})n$  has been accurately measured at  $E_{\text{cm}}=4.4$  MeV. The angular distribution for the elastic scattering cross-section  $^7\text{Be}+d$  has also been measured to extract the optical model parameters. Preliminary estimate of the spectroscopic factor  $S_{17}(0)$  is  $\sim 19 \pm 1$  ev-barn which is weakly sensitive to the optical model parameters.

In a separate measurement, preliminary estimate of the  $^7\text{Be} + ^7\text{Li}$  elastic scattering cross-section has been carried out to study the importance of charge-exchange mechanism for interaction between mirror nuclei. An in-vacuum target transfer system has been developed for making  $^7\text{Li}$  targets by vacuum-evaporation and subsequent transfer to the secondary target position in HIRA.

The neutron detector array funded by DST has now been fully commissioned and an electronic module has been designed for  $n-\gamma$  pulse-shape discrimination. Neutron spectra from the fusion reactions  $^{12}\text{C}+^{64}\text{Zn}$  at 85 MeV and  $^{31}\text{P}+^{45}\text{Sc}$  at 112 and 120 MeV have been measured in two series of complementary experiments using the time of flight method. Energy and time response for stilbene crystal for proton energies 5-25 MeV have been investigated by pulse-shape discrimination technique.

Fission fragment anisotropy for the reaction  $^{12,13}\text{C} + ^{235}\text{U}$  at near and sub-barrier energies have been studied using detector telescopes. In a separate measurement, fission fragment mass distribution in the reactions  $^{16}\text{O} + ^{209}\text{Bi}$ ,  $^{19}\text{F} + ^{209}\text{Bi}$  has been investigated to understand the role of fission dynamics in spherical nuclei.

Complete and Incomplete Fusion Reactions in  $^{12}\text{C} + ^{59}\text{Co}$ ,  $^{16}\text{O} + ^{159}\text{Tb}$  and  $^{16}\text{O} + ^{169}\text{Tm}$  have been studied at  $E_{\text{cm}} < 7$  MeV/A via excitation functions and recoil range distribution measurements. The analysis of the RRD data has indicated substantial contribution from the ICF of the incoming projectiles.

Nuclear g-factor for the  $9/2^-$  and  $21/2^-$  isomeric States in  $^{175}\text{Ta}$  have been carried out using the Perturbed Angular Correlation facility at NSC. These measurements indicate the increasing trend of g-factor from  $^{171}\text{Ta}$  to  $^{175}\text{Ta}$  nuclei for the corresponding states.

### 5.1.1 Investigation of the shears mechanism in $^{112}\text{Sb}$

A. Y. Deo<sup>1</sup>, S. K. Tandel<sup>1</sup>, S. B. Patel<sup>1</sup>, P. V. Madhusudhana Rao<sup>2</sup>, R. P. Singh<sup>3</sup>, R. Kumar<sup>3</sup>, S. Muralithar<sup>3</sup> and R. K. Bhowmik<sup>3</sup>

<sup>1</sup>Dept. of Physics, University of Mumbai, Vidyanagari, Mumbai - 400 098

<sup>2</sup>Dept. of Nuclear Physics, Andhra University, Visakhapatnam - 530 003

<sup>3</sup>Nuclear Science Centre, New Delhi - 110 067

The discovery of bands comprising M1 transitions in nuclei around  $^{200}\text{Pb}$  [1, 2] indicated the existence of a hitherto unknown excitation mechanism in nuclei. These bands show the following properties: i) the states in the bands follow rotation-like behaviour despite low deformation, ii) the levels are linked with strong M1 transitions and missing or very weak E2 transitions and iii) the ratio  $\mathfrak{I}^{(2)}/B(E2)$  is roughly an order of magnitude greater than that for normal or superdeformed bands, where  $\mathfrak{I}^{(2)}$  is moment of inertia, indicating that a substantial portion of the moment of inertia is generated from effects other than quadrupole collectivity [3]. The interpretation of this behaviour was given in terms of a new type of excitation mode [4, 5, 6], called 'Magnetic Rotation'. In the  $A \approx 110$  region, the bands are based on configurations involving high- $\Omega$   $g_{9/2}$  protons and low- $\Omega$   $h_{11/2}$  neutrons. At the bandheads these angular momentum vectors are perpendicular to each other and gradually align with the total angular momentum vector to increase the rotational frequency. This gives the physical interpretation of "Shears Mechanism". The Tilted Axis Cranking (TAC) model [4] provides the theoretical framework for the description of Magnetic Rotation and predicts such bands in the region  $A \approx 110$  [7-9] and  $A \approx 140$  [10], besides the Pb region.

The experiment to study the shears bands in  $^{112}\text{Sb}$  was performed at Nuclear Science Centre (NSC), New Delhi. The  $^{112}\text{Sb}$  nucleus was populated using the reaction  $^{89}\text{Y}(^{30}\text{Si}, 2p5n)^{112}\text{Sb}$  at a projectile energy of 120 MeV. The target used was 500  $\mu\text{g}/\text{cm}^2$  of natural yttrium deposited on 10  $\text{mg}/\text{cm}^2$  of gold backing. Five Compton suppressed Clover detectors from the Indian National Gamma Array (INGA) were used along with 2 HPGe without Compton suppression. The data were acquired using CANDLE, an acquisition system developed at NSC, with the software running on the Linux platform. The data were sorted into 4k $\times$  4k matrices using the same software, after performing a proper calibration. One-dimensional spectra were extracted from these matrices for the "LINESHAPE"[11] analysis.

The structure of  $^{112}\text{Sb}$  has been extensively studied by G. J. Lane *et al.* [12] using the Stony Brook and Eurogam-II arrays. However, the lifetime information is lacking. Using the DSAM technique, we have attempted to measure the lifetimes of a few states in one of the  $\Delta I=1$  bands, viz. band 4 in [12]. This band is based on the  $\pi g_{9/2}^{-1} \otimes \nu h_{11/2}$  configuration. According to the calculations based on geometrical model of Dönau [13], there is a characteristic decrease in the  $B(M1)/B(E2)$  ratios for this band [12]. The present study will help in determining the  $B(M1)$  values. A gradual decrease in the  $B(M1)$  values would be a signature of magnetic rotation.

The figures show a couple of representative spectra obtained during the present experiment. The gate on 202 keV shows the 326 keV, 354 keV, 381 keV and 392 keV transitions de-exciting the  $10^-$ ,  $11^-$ ,  $12^-$  and  $13^-$  states, respectively (Fig. 1). The experimental shapes for 326 keV and 392 keV transitions are also shown (Fig. 2). The detailed line shape analysis is in progress.

The authors would like to thank the Pelletron crew at the Nuclear Science Centre for the excellent support provided during the run. The help from Mr. Abhilash and Mr. Kabiraj in preparing the target is gratefully acknowledged. Also, we are thankful to Mr. P. Sugathan, Mr. J.J. Das, Mr. A. Jhingan, Mr. N. Madhavan and Mr. Thomas for their help during the run. AYD would like to acknowledge the Board of Research in Nuclear Sciences, India for the award of a research fellowship.

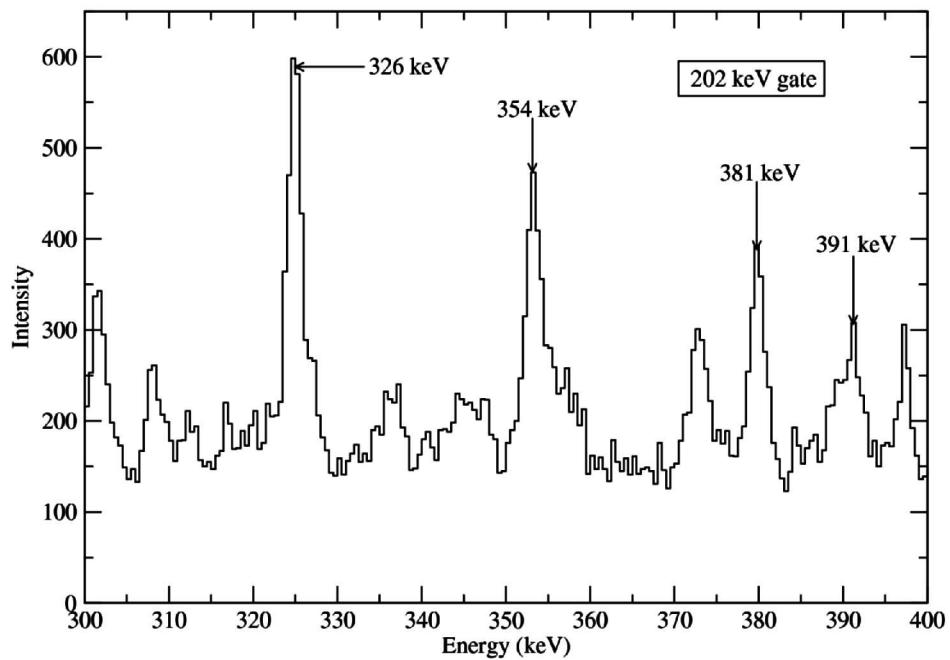


**Fig. 1 :** Partial  $\gamma$ - $\gamma$  coincidence spectra for  $^{112}\text{Sb}$  as seen in the gate on the 202keV  $\gamma$ -ray

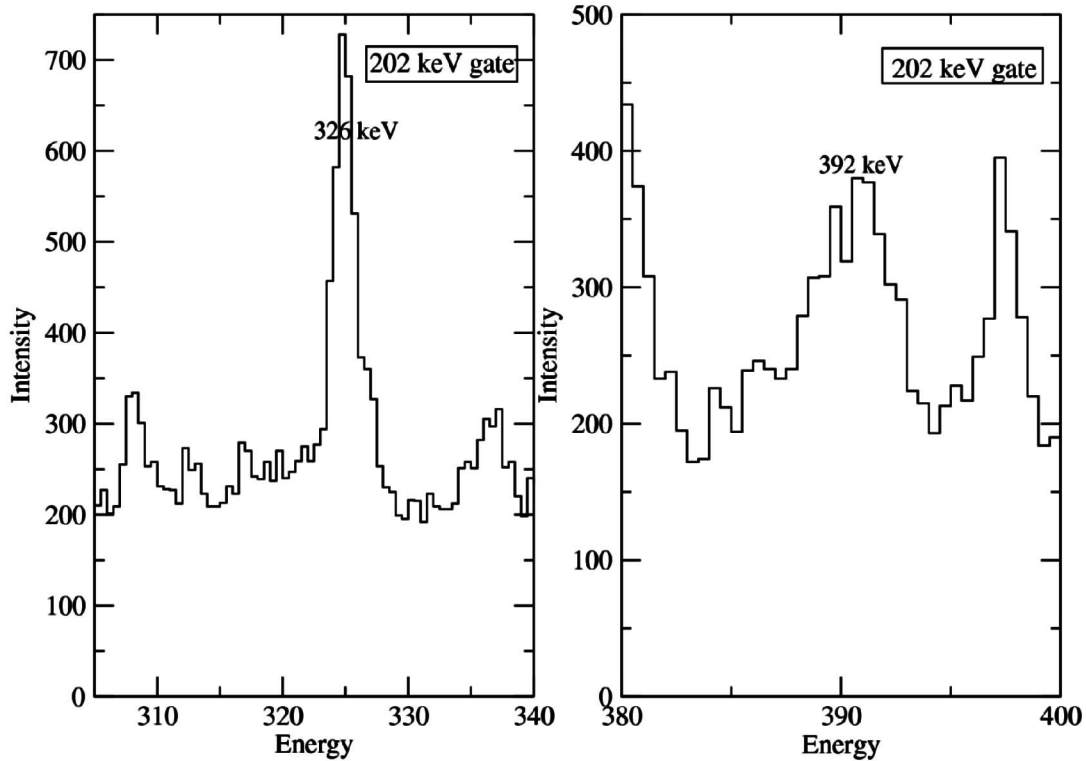


Fig. 2 : Experimental shapes of 326 keV and 392 keV transitions as seen in the gate on the 202 keV  $\gamma$ -ray

## REFERENCES

14. G. Baldsiefen *et al*, Nucl.Phys.A **574**, 521(1994)
15. M. Neffgen *et al*, Nucl.Phys.A **595**, 499(1995)
16. R. M. Clark, S. J. Asztalos *et al*, Phys. Rev. Lett. **78**, 1868 (1997)
17. S. Frauendorf *et al*, Nucl. Phys. A **557**,259c (1993)
18. S. Frauendorf, in report No. LBL - 45687, vol. 2, p. 52
19. S. Frauendorf, Proc. of Workshop on Gammasphere Physics, December 1-2, 1995, Berkeley USA
20. A. Gadea *et al*, Phys. Rev. C **55**, R1 (1997)
21. S. Frauendorf, Nucl. Phys. A **621**, 736 (1997)
22. D. G. Jenkins *et al*, Phys. Lett. B **428**, 23 (1998)
23. F. Brandolini *et al*, Phys. Lett. B **388**, 468(1998)
24. J.C. Wells (*private communication*).
25. G. J. Lane, D. B. Fossan *et al*, Phys. Rev. C **58**, 127 (1998)
26. F. Döna, Nucl. Phys. A **471**, 469 (1987)

### 5.1.2 In beam $\gamma$ -ray spectroscopy of $^{125,126}\text{Cs}$

Kuljeet Singh<sup>1</sup>, D. Mehta<sup>1</sup>, K. P. Singh<sup>1</sup>, N. Singh<sup>1</sup>, R. P. Singh<sup>2</sup>, S. Muralithar<sup>2</sup>, N. Madhavan<sup>2</sup>, J.J. Das<sup>2</sup>, S. Nath<sup>2</sup>, A. Jhingan<sup>2</sup>, P. Sugathan<sup>2</sup>, and R.K. Bhowmik<sup>2</sup>.

<sup>1</sup>Department of Physics, Panjab University, Chandigarh - 160 014

<sup>2</sup>Nuclear Science Centre, New Delhi- 110 067.

The nuclei in A=130 mass-region are known to be  $\gamma$ -soft and their shapes are strongly influenced by the quasiparticles in the high-j orbitals. The valence protons, which are in the lower part of the shell, drive it towards the prolate shape ( $\gamma = 0^\circ$ ), while the neutrons, which are in the upper part of the shell, drive it towards collective shape ( $\gamma = -60^\circ$ ). The interplay between collective and single-particle motion may very well be demonstrated at the extreme high-spin end of rotational bands, when the angular momentum reaches that of the sum of the valence nucleons outside a closed shell or subshell, the nucleons align their spins and the mass distribution changes from prolate to oblate. This change may be sudden, leading to an abrupt band termination, or it may be smoother, resulting in a soft termination with a gradual change in the moments of inertia.

In beam  $\gamma$ -ray spectroscopy in  $^{125,126}\text{Cs}$  was performed following the population through the fusion-evaporation  $^{100}\text{Mo}(^{30}\text{Si}, \text{pxn})$  reaction at 135 and 138 MeV.  $^{30}\text{Si}$  beam was delivered by the 15 UD Pelletron at NSC, New Delhi. A thick foil of  $^{100}\text{Mo} \sim 3 \text{ mg/cm}^2$  with  $15 \text{ mg/cm}^2$  lead backing was used as target. Emitted  $\gamma$ -rays were detected using INGA set up consisting of six clovers. Data analysis primarily includes building of the level scheme and determination of multi-polarities of the transitions.

#### $^{125}\text{Cs}$ :

Low-lying states in  $^{125}\text{Cs}$  have previously been determined following the  $\beta$ -decay of  $^{125}\text{Ba}$  by Arlt et al. [1] and coincident  $\gamma$ -rays have been reported by Hughes *et al.* [2]. Several rotational structures have been populated and observed in  $^{125}\text{Cs}$ . Single quasiparticle bands based on proton  $h_{11/2}$ ,  $g_{7/2}$  and proton-hole  $g_{9/2}$  orbitals, along with multi-quasiparticle bands involving  $h_{11/2}$  neutron alignment and  $\pi g_{7/2} \otimes \nu g_{7/2} \otimes \nu h_{11/2}$  structures are identified.

#### $^{126}\text{Cs}$ :

More recently, intriguing nuclear structure effects associated with spontaneous chiral symmetry breaking have been predicted from angular momentum coupling considerations in odd-odd nuclei having triaxial shapes. These predictions relate to configurations where the angular momenta of the valence proton, the valence neutron

and the core rotation are mutually perpendicular. Since, these new types of rotational bands have been predicted to exist in nuclei with stable triaxial shapes, the nuclei in the  $A=130$  region are good candidates to look for [3]. In the preliminary analysis five high-spin band structures have been observed. The yrast band is based upon  $\pi h_{11/2} \otimes \nu h_{11/2}$  configuration. Also low-spin signature inversion had been suggested in  $^{126}\text{Cs}$ .

## REFERENCE

27. P. Arlt, A. Jasinski, W. Neubert, and H.G. Ortlepp, Acta Phys. Pol. B6 (1975) 433.
28. J. R. Hughes, D. B. Fossan, D. R. LaFosse, Y. Liang, P. Vaska, and M. P. Waring, Phys. Rev. C 44 (1991) 2390.
29. K. Starosta et al., Phys. Rev. Lett. 86 (2001) 971.

### 5.1.3 Spectroscopy of Light Neutron Rich Nuclei ( $^{35}\text{P}$ , $^{36}\text{S}$ , $^{34}\text{Si}$ ..) using the nucleon transfer in Near Barrier & Sub-Barrier Heavy Ion Reactions

Anagha Chakraborty<sup>1</sup>, Krishichayan<sup>1</sup>, N.S. Pattabiraman<sup>1</sup>, S. Ray<sup>1</sup>, S.S. Ghugre<sup>1</sup>, R. Goswami<sup>1</sup>, Anukul Dhal<sup>5</sup>, Rishi Kumar Sinha<sup>5</sup>, B.K. Yogi<sup>4</sup>, L. Chaturvedi<sup>5</sup>, S. Saha<sup>2</sup>, M.B. Chatterjee<sup>2</sup>, S.K. Basu<sup>3</sup>, R. Singh<sup>6</sup>, P.V. Madhusudhana Rao<sup>7</sup>, A. Jhinghan<sup>7</sup>, R.P. Singh<sup>7</sup>, S. Muralithar<sup>7</sup>, N. Madhavan<sup>7</sup>, P. Sugathan<sup>7</sup>, J.J. Das<sup>7</sup>, S. Nath<sup>7</sup>, A.K. Sinha<sup>1</sup> and R.K. Bhowmik<sup>7</sup>

<sup>1</sup>Inter University Consortium for DAE Facilities, Calcutta Center, Kolkata-98

<sup>2</sup>Saha Institute of Nuclear Physics, Sector I-AF, Bidhan Nagar, Kolkata

<sup>3</sup>Variable Energy Cyclotron Center, Sector I-AF, Bidhan Nagar, Kolkata

<sup>4</sup>Government College, Kota

<sup>5</sup>Department of Physics, Banaras Hindu University, Varanasi, 221 005

<sup>6</sup>Department of Physics and Astrophysics, Delhi University, Delhi

<sup>7</sup>Nuclear Science Center, New Delhi 110 067

Exploration of the nuclear structure of hard to access neutron rich nuclei in the mass region  $A \sim 30 - 40$  has revealed several intriguing aspects of nuclear structure even at low spins. However, since these nuclei are not accessible using the conventional evaporation reactions information on these nuclei is extremely scarce. These nuclei could be investigated only via other modes of decay such as single or multi-nucleon transfer reactions etc. Some of the interesting phenomena in these nuclei could be summarized as follows

30. Co-existence between spherical and deformed configurations.
31. Role of the  $f_{7/2}$  intruder orbital (especially when the level has low occupation) similar to the role of  $g_{9/2}$  orbital in the  $A \sim 90$  region.

32. The overlap of the proton  $d_{5/2}$  and the neutron  $d_{3/2}$  and  $f_{7/2}$  orbital could stabilize deformed shapes even at modest spin and excitation energies.

At incident energies around the barrier where the formation of compound nucleus is inhibited but the projectile interacts with the target to exchange one or few nucleons before flying apart. Thus making it possible to populate and study neutron rich nuclei.

An attempt was undertaken to investigate the level structure of nuclei around  $A \sim 30 - 40$  using the  $^{34}\text{S} + ^{115}\text{In}$  reaction @ 150 – 160 MeV at Nuclear Science Centre using the Indian National Gamma Array (INGA). We have carried out an exploratory experiment using two targets (i) 75 mg/cm<sup>2</sup> thick self-supporting  $^{115}\text{In}$  target and (ii) 1.29 mg/cm<sup>2</sup> thick  $^{115}\text{In}$  target with Au ( $\sim 7.14$  mg/cm<sup>2</sup>) thick backing. For the second target the Au was kept facing the beam, so that back-scattered projectile like fragments would be stopped in the backing. The forward-scattered projectile like fragments, moving with almost the beam velocity, would not be stopped in the target.

A modest 4 clover array was employed to detect the de-exciting gamma rays. The preliminary analysis of the coincidence gamma spectrum indicated, apart from the nuclei produced in fusion-evaporation reaction, the population of  $^{114}\text{In}$  (complimentary projectile like fragment of  $^{35}\text{S}$ ),  $^{115}\text{Sn}$  (complimentary projectile like fragment of  $^{34}\text{P}$ ),  $^{116}\text{Sn}$  (populating through the one proton stripping reaction, complimentary projectile like fragment of  $^{33}\text{P}$ ). The  $\gamma$ -lines from the projectile-like fragments (i.e.  $^{35}\text{S}$ ,  $^{33,34}\text{P}$ ) however could not be identified from the present experiment. A separate experiment is planned to directly detect the target-like fragments in the recoil separator HIRA.

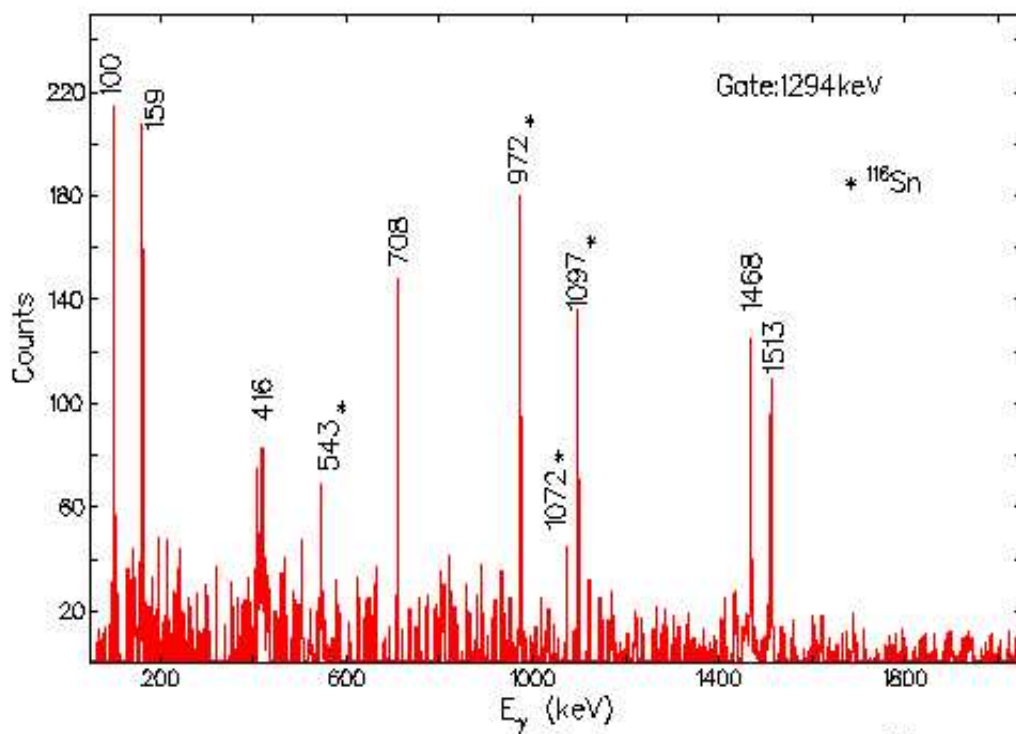


Fig. 1 :  $\gamma$  - spectrum gated by  $2^+ \rightarrow 0^+$  transition in  $^{116}\text{Sn}$  (complementary TLF of  $^{33}\text{P}$ )

#### 5.1.4 Study of High Spin States In $^{138}\text{Ce}$

S. Chanda<sup>1</sup>, A. Mukherjee<sup>2</sup>, S.K. Basu<sup>2</sup>, S. Bhattacharyya<sup>2</sup>, T. Bhattacharjee<sup>2</sup>, S.S. Ghugre<sup>3</sup>, U. Datta Pramanik<sup>4</sup>, R.P. Singh<sup>5</sup>, S. Muralithar<sup>5</sup>, N. Madhavan<sup>5</sup>, J.J. Das<sup>5</sup> and R.K. Bhowmik<sup>5</sup>

<sup>1</sup>Fakir Chand College, Diamond Harbour, W. B., India

<sup>2</sup>Variable Energy Cyclotron Centre, Kolkata, W. B., India

<sup>3</sup>Inter University Consortium for DAE Facilities, Kolkata, W. B., India

<sup>4</sup>Saha Institute of Nuclear Physics, Kolkata, W. B., India

<sup>5</sup>Nuclear Science Centre, New Delhi-110 067

As a part of our ongoing project on the studies of high spin states in  $N=80$  nuclei close to  $A = 140$ , we have investigated the  $^{138}\text{Ce}$  nucleus using the reaction  $^{130}\text{Te}(^{12}\text{C}, 4n)^{138}\text{Ce}$  at  $E_{\text{lab}} = 65$  MeV. The  $^{12}\text{C}$  beam was obtained from the 15UD Pelletron accelerator at NSC, New Delhi. We used a  $2.2$  mg/cm<sup>2</sup> thick metallic  $^{130}\text{Te}$  (99.99%) target, evaporated on a  $2.0$  mg/cm<sup>2</sup> Au foil and it was covered by a  $50\mu\text{g}/\text{cm}^2$  thin Au film from top. As predicted by the PACE2 calculations, the dominant evaporation channels in this reaction were  $^{137,138,139}\text{Ce}$ , of which the yield of  $^{138}\text{Ce}$  was maximum. The gamma rays from the decaying states in the residual nuclei were studied by the Indian National Gamma Array (INGA), capable of accommodating eight HPGe Clover detectors. The

support structure of this array is so designed that two sets of four clover detectors are sitting at  $81^\circ$  and  $141^\circ$  respectively. For the present experiment, only five out of eight Clovers were available. Out of these, two were put in the forward hemisphere and the rest were put in the backward hemisphere. Apart from these, there were two single crystal HPGe (23%) detectors sitting at  $\pm 10^\circ$  in the forward hemisphere. Signals from three clover detectors were processed using the conventional NIM electronics, whereas the energy and the timing signals from two clovers were processed by using an indigenously developed module, developed by NSC group in which four energy and timing channels have been integrated [1]. The ‘master gate’ was generated with the condition of  $M\gamma \geq 2$ , where  $M\gamma$  is the ‘gamma multiplicity’ defined by the number of clovers fired in a single event within a time window of  $\sim 200$  ns. There are two isomeric states at 2.13 MeV and 3.54 MeV in  $^{138}\text{Ce}$  [2] with half lives of 8.65 ms and 81 ns respectively. The decay gamma rays from those isomers also contribute randomly to the ‘master’ signal; however, it is observed that most of the time only prompt gamma rays contribute. As a matter of fact, we can generate a  $\gamma\gamma$  TAC in offline analysis of the list data and certainly can put a “prompt time window” in order to generate a prompt  $E\gamma$ - $E\gamma$  matrix. With this aim in mind,  $\gamma\gamma$  coincidence data were acquired using the NSC developed LINUX based acquisition software “CANDLE” [3], which has built-in features of multi-crate acquisition. With this set-up, we collected  $\sim 350$  million two and higher fold coincidence data (prompt as well as delayed), which is being analyzed currently using a modified version of the program “NSCSORT”, popularly called as “INGASORT” [4]. This program is able to unfold the triples events into doubles and produce  $\gamma\gamma$  matrix after appropriate gain matching. In figs. (1) and (2) some representative coincidence spectra, corresponding to the strongest channel, are shown. The level scheme of  $^{138}\text{Ce}$  has been considerably extended and is being rechecked through an analysis of  $\gamma\gamma\gamma$  CUBE using the program IUCSORT [5].

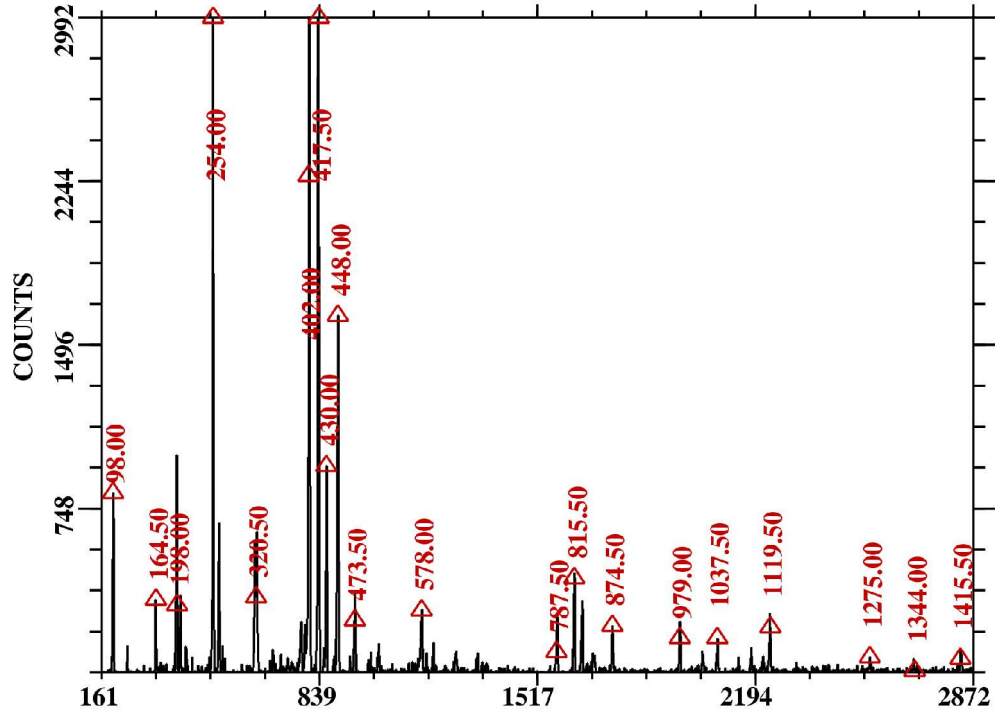


Fig. 1 : 854 keV gate in  $^{138}\text{Ce}$  using background subtracted  $E\gamma$ - $E\gamma$  matrix

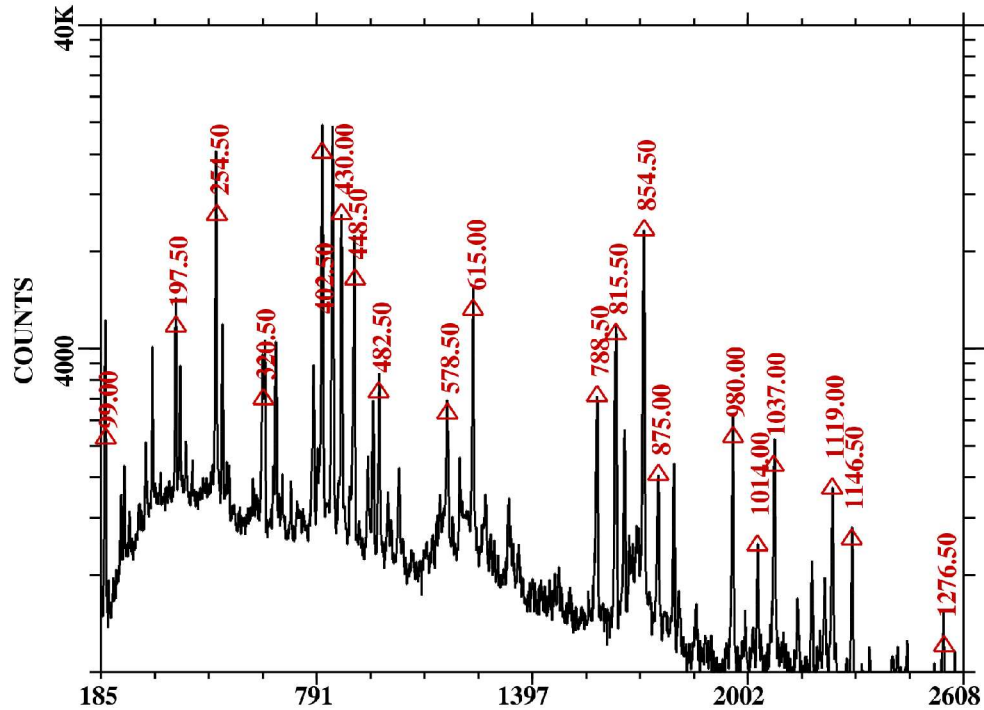


Fig. 2 : 403+417+854 keV added gate, showing gamma-rays from the highest spin state in the ground state band

## REFERENCES

33. S. Venkataramanan et al, Proc. of the DAE Symp. on Nucl. Phys., 45B (2002), p.420
34. J. R. Leigh et al, Nucl. Phys. A213 (1973) 1; M. Kortelahti et al, Nucl. Phys. A376 (1982) 1
35. R. K. Bhowmik, Private communication (2002)
36. R. K. Bhowmik et al, Proc. of the DAE Symp. on Nucl. Phys, 44B (2001), p.422
37. S. S. Ghugre, Proc. of the DAE Symp. on Nucl. Phys, 44B (2001), p.25

### 5.1.5 Study of n-p interaction in $N = Z$ Nuclei in mass 80 region

H.C. Jain<sup>1</sup>, P.K. Joshi<sup>1</sup>, I. Mazumdar<sup>1</sup>, S. Lakshmi<sup>1</sup>, H.V. Panchal<sup>1</sup>, S. Nagraj<sup>1</sup>, B.S. Naidu<sup>1</sup>, S. Chattopadhyay<sup>2</sup>, J.J. Das<sup>3</sup>, K.S. Golda<sup>3</sup>, A. Jhingan<sup>3</sup>, Rakesh Kumar<sup>3</sup>, N. Madhavan<sup>3</sup>, P.V. Madhusudhana Rao<sup>3</sup>, S. Murlithar<sup>3</sup>, Subir Nath<sup>3</sup>, R.P. Singh<sup>3</sup>, P. Sugathan<sup>3</sup> and R.K. Bhowmik<sup>3</sup>

<sup>1</sup>Tata Institute of Fundamental Research, Colaba, Mumbai 400 005

<sup>2</sup>Saha Institute of Nuclear Physics, Bidhan Nagar, Kolkata

<sup>3</sup>Nuclear Science Center, New Delhi-110 067

There has been considerable interest in recent years in investigating the effects or the signature of n-p interaction in nuclei. n-p interaction has maximum influence on nuclear properties in  $N=Z$  nuclei since the Fermi surfaces for neutrons as well as protons are quite close to each other i.e. the valence nucleons occupy the same orbitals and are, therefore, likely to have stronger interaction compared to  $N=Z+2$  or  $Z+4$  nuclei. It is, therefore, quite attractive to study the properties of  $N=Z$  nuclei to search for the fingerprints of n-p interaction. In addition to studying  $N=Z$  nuclei, it is necessary to choose a nuclear property that will be sensitive to increase/decrease in n-p interaction strength and also select a mass region most suitable for these studies.

Mass-80 region has provided an excellent testing ground for nuclear properties during last 10-15 years. This is due to relatively small level density compared to, for example, the rare earth region. This leads to large variations in nuclear properties with changes in nucleon numbers by 1 or 2. Thus, the variation in some nuclear property in  $N = Z$  and  $N = Z+2$  or 4 nuclei could be correlated to a variation in n-p interaction.  $N = Z$  nuclei in mass 70 to 80 region are produced with a small cross-section  $\sim 10$  to  $100 \mu\text{b}$ . But, the present day experimental techniques have made it possible to study the properties of nuclei produced with the small cross-sections mentioned above to quite high angular momenta. So any effect of n-p interaction showing up at high angular momentum can be investigated.

An interesting phenomenon reported recently is the observed delay in the band-crossing frequencies in the  $N = Z$  nuclei compared to the  $N = Z+2$  or  $Z+4$  nuclei in Kr, Sr and Zr isotopes. The possibility of the n-p pairing being responsible for delayed band crossings in  $N = Z$  nuclei has been addressed both theoretically as well as experimentally

recently. It is well known that the pairing correlations in nuclei reduce the moment of inertia of deformed nuclei by about a factor of 2 compared to the rigid body value. The effect of Coriolis forces is to reduce the effect of pairing correlations – thus leading to an increase in moment of inertia with increasing rotational frequency. There are theoretical models [1- 4], which calculate the frequency where pairs break. In heavy nuclei, pairs of identical nucleons exist in time reversed orbitals coupled to  $J = 0^+$ , and isospin  $T = 1$ . In light nuclei with  $N = Z$ , neutron and protons are paired with  $J, T = 0, 1$  (as in ‘normal’ pairing) or an isospin anti-symmetric wave function with  $T = 0$  and  $J = 0$ , or both. One of the possibility investigated is that the  $T = 0$  pairs are more robust and less easily destroyed by the Coriolis forces.  $T = 0$  pairing may, therefore, be more important at higher angular momentum where other correlations have already quenched. Recent advances in experimental techniques have made possible the spectroscopic studies along  $N = Z$  line between  $^{56}\text{Ni}$  and  $^{100}\text{Sn}$ . It is for this reason that considerable interest has been focussed on the issue of n-p pairing. The  $T = 0$  pairing will lead to a delay in the irregularities due to alignments or backbends in moment of inertia vs. frequency plots [5,6] or the irregularities may disappear altogether. Recently, the absence of a band crossing in the yrast band of  $^{72}\text{Kr}$  [7] has been interpreted [4,8] as arising due to stronger n-p interaction in  $N=Z$  nuclei compared to  $N= Z+2, Z+4$  nuclei. The present experiment was aimed at extending the yrast band of the  $N=Z$  nucleus  $^{84}\text{Mo}$  to obtain the band crossing frequency in this nucleus.

### Experimental set up and results

Energy levels in  $^{84}\text{Mo}$  were populated by bombarding 92 MeV  $^{28}\text{Si}$  beam from the 15-UD Pelletron at Nuclear Science Centre on an enriched  $450 \mu\text{g}/\text{cm}^2$  thick  $^{58}\text{Ni}$  foil. The reaction channel of interest i.e.  $^{84}\text{Mo}+2n$  has a small cross section  $\sim 10 \mu\text{b}$ . Relatively stronger channels in this reaction accounting for more than 200 mb cross section are:  $^{84}\text{Nb}+pn$ ,  $^{84}\text{Zr}+2p$ ,  $^{83}\text{Y}+3p$ ,  $^{83}\text{Zr}+2pn$ ,  $^{83}\text{Nb}+p2n$ ,  $^{81}\text{Zr}+\alpha n$ .  $\gamma$  spectroscopy of  $^{84}\text{Mo}$  through the  $^{28}\text{Si}+^{58}\text{Ni}$  requires the suppression of the  $\gamma$  background due to stronger reaction channels. This has been achieved in the present experiment through the use of :

38. ‘Heavy Ion Reaction Analyser (HIRA)’ for selecting reaction products with mass  $A=84$ ,
39.  $4\pi$  charge particle ball obtained from TIFR gave the proton multiplicity spectrum – the idea has been to reject an event in which a proton is emitted,
40. Four neutron detectors with liquid scintillator cells with 5”dia x 5” thickness were used for selecting channels with neutron emission.

$\gamma\gamma$  coincidences were obtained with Indian National Gamma Array (INGA) array jointly set up by TIFR, NSC, SINP and IUC-DAEF. 8 clover were placed at  $80^\circ$  and  $140^\circ$  with respect to the beam direction. Two-fold  $\gamma$ - $\gamma$  coincidences were used as masters and list mode data were obtained with 42 parameters i.e. parameters 1 to 32 registered 32  $\gamma$

spectra from 32 crystals in 8 clovers, par 33: mass spectrum from HIRA, par 34: charge particle multiplicity, par 35 to 38: n- $\gamma$  discrimination spectra, par 39:  $\gamma$ - $\gamma$  time spectrum, par 40: M- $\gamma$  time spectrum, par 41: CPB- $\gamma$  time spectrum and finally par 42: n- $\gamma$  time spectrum. The beam current varied between 60 nA to 120 nA over a period of 12 days. A total of 900 million events have been collected in this experiment.

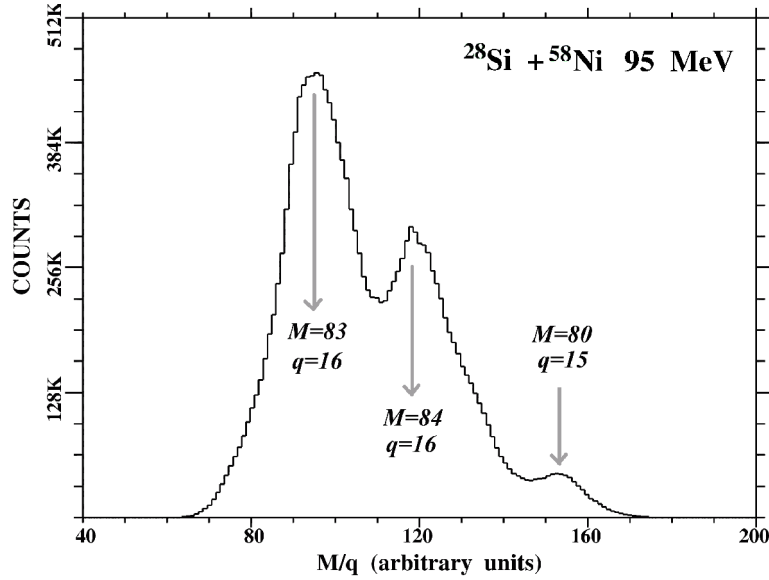


**Fig. 1 : M/q spectrum in the focal plane detector**

The mass spectrum at the HIRA focal plane detector is shown in Fig. 1. Three M/q groups corresponding to  $M = 83$   $q = 16$ ,  $M = 84$   $q = 16$  and  $M = 80$   $q = 15$  can be identified in the mass spectrum. The line shapes for individual mass groups were obtained by gating the mass spectrum by known lines in the nuclei  $^{80}\text{Sr}$ ,  $^{83}\text{Y}$  and  $^{84}\text{Zr}$  (Fig. 2). Other mass groups populated in the reaction fall outside the acceptance window of the recoil separator.

**Fig. 2 : M/q spectra gated by known transitions in  $^{80}\text{Sr}$ ,  $^{83}\text{Y}$  and  $^{84}\text{Zr}$ . The heights for different mass groups have been arbitrarily normalised**

**Fig. 3 : Mass-gated energy spectra from a  $\gamma$ - detector at  $80^\circ$ . Energy levels corresponding to  $^{84}\text{Zr}$  (in A=84 gate) and  $^{83}\text{Y}$  (in A=83gate) are marked. The  $\gamma$ -energies have been corrected for Doppler shift. For clarity, the upper spectrum has been multiplied by a factor of 50 w.r.t. the bottom spectrum**

Fig. 3 shows the recoil gated  $\gamma$ -energy spectra for A = 84 (bottom curve) and A = 83 (top curve). The characteristic transitions in  $^{84}\text{Zr}$  and  $^{83}\text{Y}$  are marked in the figure. The analysis of data is in progress to study level structure of mass 84, 83 and 80 nuclei.

Authors would like to thank the Pelletron operation staff of NSC for smooth operation of the accelerator and the workshop staff for their help during the experiment.

## REFERENCES

41. R. Bengtsson and S. Freundorf, Nucl. Phys. A327 (1979) 53.
42. W. Nazarewicz, J. Dudeck, R. Bengtsson and I. Rangarsson, Nucl. Phys. A435 (1985) 397.
43. W. Satula and R. Wyss, Phys. Scr. T56 (1995) 159.
44. R. Palit, J.A. Sheikh, Y. Sun and H.C. Jain, Nucl. Phys. A686 (2001) 141.
45. S. Freundorf and J.A. Sheikh, Phys.Rev. C59 (1999) 1400, Phys. Scr. T88 (2000) 162, Nucl Phys. A645 (1999) 509.
46. W. Satula and R. Wyss, Phys. Lett. B393 (1997) 1.
47. S.M. Fischer et al, Phys. Rev. Lett. 87 (2001) 132501-1.
48. Y. Sun and J.A. Sheikh, Phys. Rev. C64 (2001) 031302.

### 5.1.6 Structure studies of neutron rich nuclei in mass 100 region

P. Datta<sup>1</sup>, S. Chattopadhyay<sup>2</sup>, W. Bari<sup>2</sup>, S. Bhattacharya<sup>2</sup>, R.K Bhowmik<sup>5</sup>,  
 U. Datta Pramanik<sup>2</sup>, T. Ghosh<sup>2</sup>, A. Goswami<sup>2</sup>, H.C Jain<sup>3</sup>, P.K Joshi<sup>3</sup>,  
 N. Madhavan<sup>5</sup>, S. Muralithar<sup>5</sup>, S. Pal<sup>2</sup>, A. Rastogi<sup>4</sup>, R. Raut<sup>2</sup>, P.V. Madhusudhana  
 Rao<sup>5</sup>, R.P Singh<sup>5</sup> and M. Saha Sarkar<sup>2</sup>

<sup>1</sup>Ananda Mohan College, Kolkata 700 009

<sup>2</sup>Saha Institute of Nuclear Physics, 1/AF Bidhan Nagar, Kolkata 700 064

<sup>3</sup>Tata Institute of Fundamental Research, Mumbai 400 005

<sup>4</sup>RBS College, Agra 282 002

<sup>5</sup>Nuclear Science Centre, New Delhi-110 067

In fusion-evaporation reactions, the neutron rich nuclei of mass-100 region are produced with low cross-sections (tens of mb or less) while the residual nuclei produced through pure neutron evaporations from the compound nucleus, have much higher (about two order of magnitude) cross-sections. Thus, to carry out the gamma-gamma coincidence studies in these neutron rich nuclei an additional filter detector system is necessary which will suppress the pure neutron channels.

In the present work, the neutron rich nuclei were produced through  $^{100}\text{Mo}(^{13}\text{C},x\text{pyn})$  reaction with 65 MeV  $^{13}\text{C}$  beam from Nuclear Science Centre. The dominant evaporation channels of the reaction were  $4n$  (45% of the total cross-section) leading to  $^{109}\text{Cd}$  and  $5n$  (40%) leading to  $^{108}\text{Cd}$  channels while the neutron rich  $^{109}\text{Ag}$  corresponded to  $p3n$  channel (4%).

In order to perform the gamma-gamma coincidence study in  $^{109}\text{Ag}$ , a Phoswich Ball from Tata Institute of Fundamental Research, Mumbai was used to detect the evaporated charged particles from the compound nucleus. Thus, a coincidence with this Phoswich Ball will suppress the gamma-rays from the residual nuclei produced through pure neutron evaporations. The Phoswich Ball has 10 Phoswich scintillators which were prepared by hot pressing 0.1 mm thick NE102 on 10 mm thick NE115. These detectors were mounted on a vacuum chamber shaped in the form of a dodecahedron. The distance between the detector faces and the target was 17 mm. A cylindrical Ta absorber of  $60\text{ mg/cm}^2$  was placed between the target and Phoswich detector faces, in order to cut down the elastically scattered beam from the target.

A total list mode data of 800 million gamma-gamma coincidences were collected using Indian National Clover Array. The evaporated charged particle multiplicity was collected as a parameter in the list mode data. This data were sorted to form a gamma-gamma matrix with one proton gate and 100 ns prompt windows on both gamma-gamma and p-gamma TACs. This p-gamma-gamma matrix had 40 million events.

Fig. 1 shows the background subtracted projection of the gamma-gamma matrix (top half of the figure) and the p-gamma-gamma matrix (bottom half of the figure). It is evident from this figure that the pure neutron channels ( $^{108,109}\text{Cd}$ ) were well suppressed by the proton gate. Fig. 2 shows the level scheme of  $^{109}\text{Ag}$ , which was constructed from the p-gamma-gamma matrix. The present scheme is in good agreement with the level scheme given by Pohl et al [1].



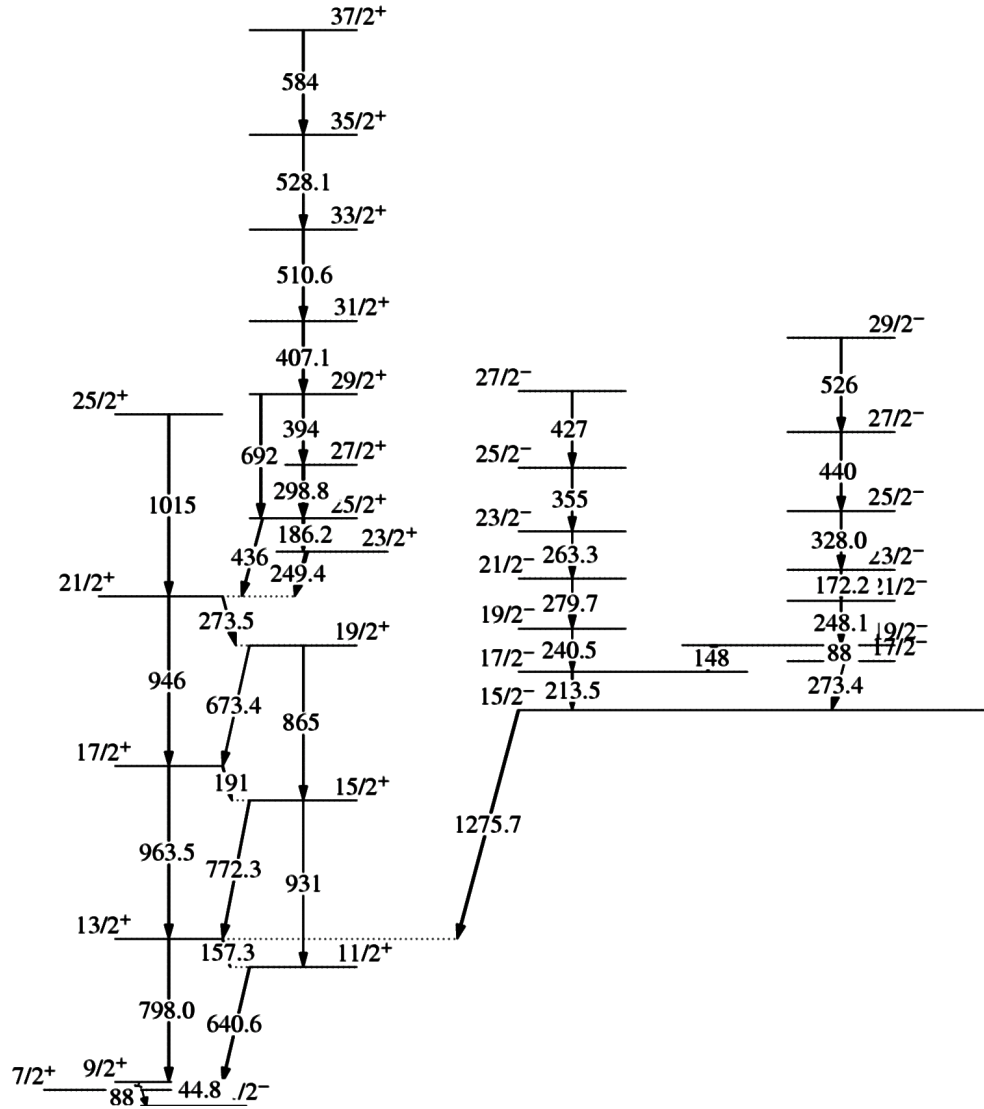


Fig. 2 : Partial level scheme of  $^{109}\text{Ag}$

## REFERENCE

49. K.R Pohl et al., Phys. Rev. C **53** (1996) 2682.

### 5.1.7 Spectroscopy of Ar and K isotopes in A=40 region

M. Saha Sarkar<sup>1</sup>, R. Raut<sup>1</sup>, S. Bhowal<sup>2</sup>, I. Roy<sup>1</sup>, S. Sarkar<sup>3</sup>, G. Ganguly<sup>4</sup>, P. Banerjee<sup>1</sup>, J. M. Chatterjee<sup>1</sup>, S. Chattaopadhyay<sup>1</sup>, U. Datta Pramanik<sup>1</sup>, A. Goswami<sup>1</sup>, S. Bhattacharya<sup>1</sup>, B. Dasmahapatra<sup>1</sup>, K.S. Golda<sup>5</sup>, R. Kumar<sup>5</sup>, R.P. Singh<sup>5</sup>, S. Muralithar<sup>5</sup>, P.V. Madhusudhana Rao<sup>5</sup>, N. Madhavan<sup>5</sup>, J.J. Das<sup>5</sup>, S. Nath<sup>5</sup>, P. Sugathan<sup>5</sup>, A. Jhingan<sup>5</sup> and R.K. Bhowmik<sup>5</sup>

<sup>1</sup>Saha Institute of Nuclear Physics, Kolkata

<sup>2</sup>Department of Physics, Surendranath College, Kolkata

<sup>3</sup>Department of Physics, Burdwan University, Burdwan

<sup>4</sup>Department of Physics, Calcutta University, Kolkata

<sup>5</sup>Nuclear Science Centre, New Delhi-110 067

Experimental data on doubly magic nuclei and their neighbours give useful information on effective nuclear force. The excitation spectra of the doubly magic  $^{40}\text{Ca}$  and several other nuclei in the neighbourhood also revealed deformed states at low-excitation energies, indicating that the nuclei near the closed shell with  $Z$  or  $N=20$  can easily lose spherical shape. Due to experimental limitations in the sensitivity and efficiency of the detection systems, mostly low spin states in proton rich nuclei in this mass region were reported in the earlier studies till late 80's. In the recent years, employment of sophisticated techniques of gamma spectroscopy permitted observation of high spin states of several nuclei. The results show that, the excitation spectra in most of these nuclei are well explained by shell - model calculations, while in a few of them states with features of permanent deformation are also observed. The recent observation of a superdeformed band in  $N=Z$   $^{36}\text{Ar}$  has generated new interest in this mass region [1].

An experiment was proposed at NSC using the INGA + the auxiliary detector setup to study  $A\sim 40$  region with the following objectives. The main interest was to study the higher spin states in  $^{38}\text{Ar}$ ,  $^{35}\text{Cl}$  and  $^{38}\text{K}$  (already studied at lower beam energy  $\sim 70$  MeV [2] in the INGA setup at TIFR) and other weaker channels like  $^{35,37}\text{Ar}$ , where heavy ion data are scanty. The auxiliary detector systems should be used to get cleaner data for the above purposes.

Very recently, the above experiment has been completed using the array of eight Clover detectors at NSC along with the ten-element charge particle detector array (CPDA provided by TIFR group) and four neutron detectors. A  $\sim 50$   $\mu\text{g}/\text{cm}^2$  C target backed by  $\sim 10.5$   $\text{mg}/\text{cm}^2$  gold was used. The beam was  $^{28}\text{Si}$  at 88 MeV. A small part of the data was analysed and its consistency was checked. The data from the neutron detectors especially were found to be very helpful in identifying the weaker channels of interest (Fig.1).

Detailed data analysis is in progress

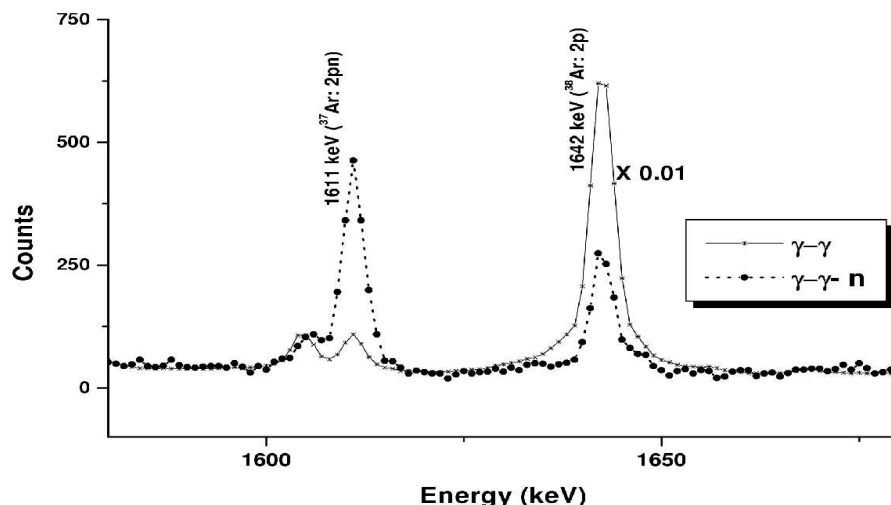


**Fig. 1 : Comparison of  $\gamma\text{-}\gamma$  total projection spectrum with that gated with neutrons**

To determine the efficiency of the gamma detectors in the present setup at higher energies (2 MeV – 5 MeV) [3], natural Chromium was irradiated with 50 MeV  $^{16}\text{O}$  beam and a radioactive source of  $^{66}\text{Ga}$  ( $T_{1/2} = 9.49$  h) was prepared. The decay of  $^{66}\text{Ga}$  gives a large number of strong gamma rays ranging from 0.833 MeV to 4.806 MeV. The irradiation was done in the GPSC for about three hours. Later the source was mounted in the target frame and efficiency data were accumulated.

## REFERENCES

50. C.E. Svensson *et al.*, Phys. Rev. Lett. 85 (2000) 2693.
51. M. Saha Sarkar, P. Datta, I. Ray, C.C. Dey, S. Chattopadhyay, A. Goswami, P. Banerjee, S. Bhattacharya, J.M. Chatterjee, S. Sen, B. Dasmahapatra, Proc. DAE- BRNS Symp. Nucl. Phys. (India) B 44 (2001) 112.
52. M. Saha Sarkar, P. Datta, I. Ray, C.C. Dey, S. Chattopadhyay, A. Goswami, P. Banerjee, R.P. Singh, P.K. Joshi, S.D. Paul, S. Bhattacharya, R. Bhowmik, J.M. Chatterjee, H.C. Jain, S. Sen and B. Dasmahapatra, Nucl. Instr. & Meth. A491 (2002) 113.

### 5.1.8 Investigations of low and high spin states of $^{134}\text{La}$

Vinod kumar<sup>1</sup>, Pragma Das<sup>1</sup>, R.P. Singh<sup>2</sup>, S. Muralithar<sup>2</sup> and R.K. Bhowmik<sup>2</sup>

<sup>1</sup>Physics Department, India Institute of Technology-Bombay, Mumbai

<sup>2</sup>Nuclear Science Centre, New Delhi-110 067

The odd-odd nuclei in the mass region  $\sim 130$  has recently gained tremendous interest because of the newly recognized phenomenon of chirality. Many nuclei with  $N = 73, 75$  and  $Z = 55, 57, 59$  and  $61$  have now been experimentally known to exhibit chiral rotation. Among  $N = 77$  isotones the experimental data on  $^{134}\text{La}$  indicated the existence of chiral partner band by Bark *et al.*, [1]. The intensity of this band was very weak and

the number of energy levels belonging to the band were very few in number. Therefore, their claim was only tentative. We began our investigations on  $^{134}\text{La}$  with the primary aim of making the existence or non-existence of the chiral partner band more definite. The motivation was also to study the nuclear structure of many other low and high spin states.

An experiment using the fusion evaporation reaction  $^{124}\text{Sn}(^{14}\text{N}, 4n) ^{134}\text{La}$  was performed using the Gamma Detector Array (GDA) at NSC, Delhi. The energy calibration and efficiency determination of each detector was done using the radioactive sources  $^{133}\text{Ba}$  and  $^{152}\text{Eu}$ . After the excitation function measurement, the list mode data for the  $\gamma\text{-}\gamma$  coincidence were collected at the beam energy 65, 67 and 70 MeV. A total of approximately  $7.5 \times 10^8$   $\gamma\text{-}\gamma$  coincidence events were collected.

In order to analyze the experimental data, the entire list mode data were first calibrated. A  $E_{\gamma^-} E_{\gamma^+}$  matrix was then constructed using the computer program "FREEDOM" [2]. The slices for the known and the unknown  $\gamma$ -transitions were obtained from the symmetrised  $E_{\gamma^-} E_{\gamma^+}$  matrix. The software RADWARE [3] was utilized for this purpose. The decay scheme was built with the help of coincidence and intensity relationships between various  $\gamma$ - transitions. Figure 1 shows the projected spectrum as an example, corresponding to the gate on 285 keV transition newly found from our data. Many coincident new transitions were found and placed in the decay scheme (Fig. 1 and Fig. 2). As a result, an entirely new band was constructed.

**Fig. 1 : Level scheme of  $^{134}\text{La}$**

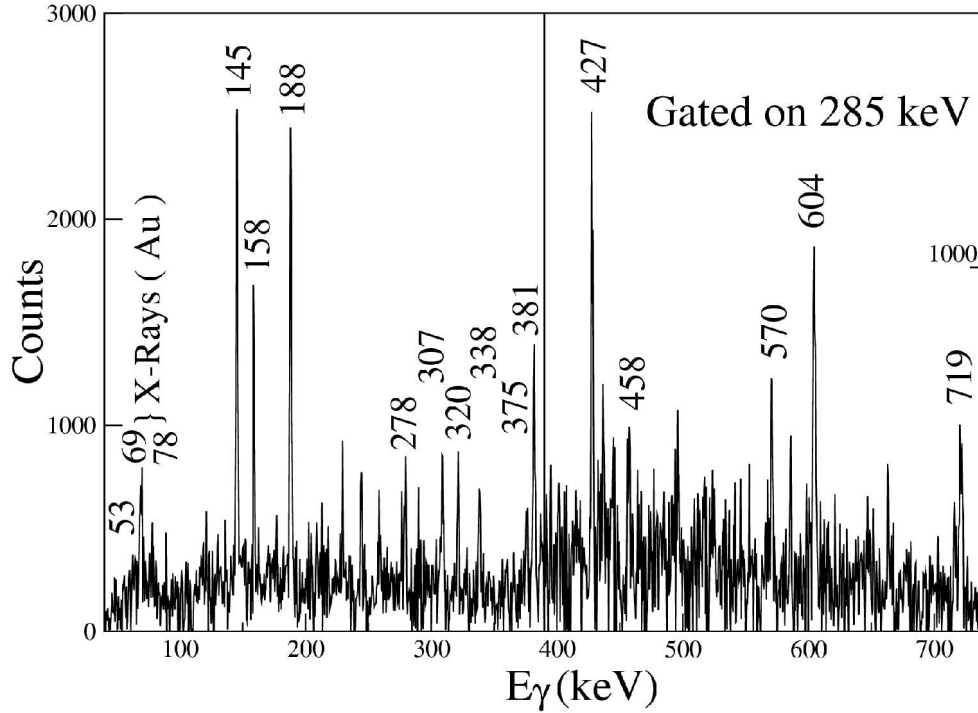


**Fig. 2 :  $\gamma$ -spectrum of  $^{134}\text{La}$  gated by 285 keV transition**

In order to determine the spins of states, the method of finding the Directional Correlation ratios (DCO) was utilized. For this purpose, an  $E_\gamma$ - $E_\gamma$  matrix was made with detectors angles of  $50^\circ$ , ( $144^\circ \equiv 36^\circ$ ), on one axis and  $98^\circ$  on the other axis. This resulted in the averaged value of the detector positions  $\theta = 98^\circ$ ,  $43^\circ$  and  $\phi = 0$ . Here ' $\phi$ ' is the angle between two detector planes, each of which was created by the detector direction and the beam direction. To determine the DCO ratios, slices were taken with gate on  $\theta = 43^\circ$ , projected on  $\theta = 98^\circ$ , and *vice versa*. The experimentally determined values of the DCO ratios were compared with the theoretical ones, to determine the multipolarity of the transition. The theory was based on the prescription given by Krane et al., [4]. Assuming the population parameter  $\sigma/I = 0.3$ , the theoretical curves were plotted as a function of the mixing ratio ' $\delta$ '. For the entire data analysis, E2 transitions were considered to be pure, i.e.  $\delta = 0$ . For the dipole transitions, the property of E1 transitions having very small mixing with M2, was occasionally exploited to assign the parity of the states. Fig.3 shows an example of DCO analysis for finding the spin of the state decaying via 285 keV transition. A very small values of  $\delta$  for the 427 keV transition was first determined by the DCO analysis of 719 keV - 427 keV coincident transitions [Fig. 3(a)]. A similar DCO analysis for 427 keV- 285 keV coincident transitions was then used to obtain the spin value I [Fig. 3 (b)].

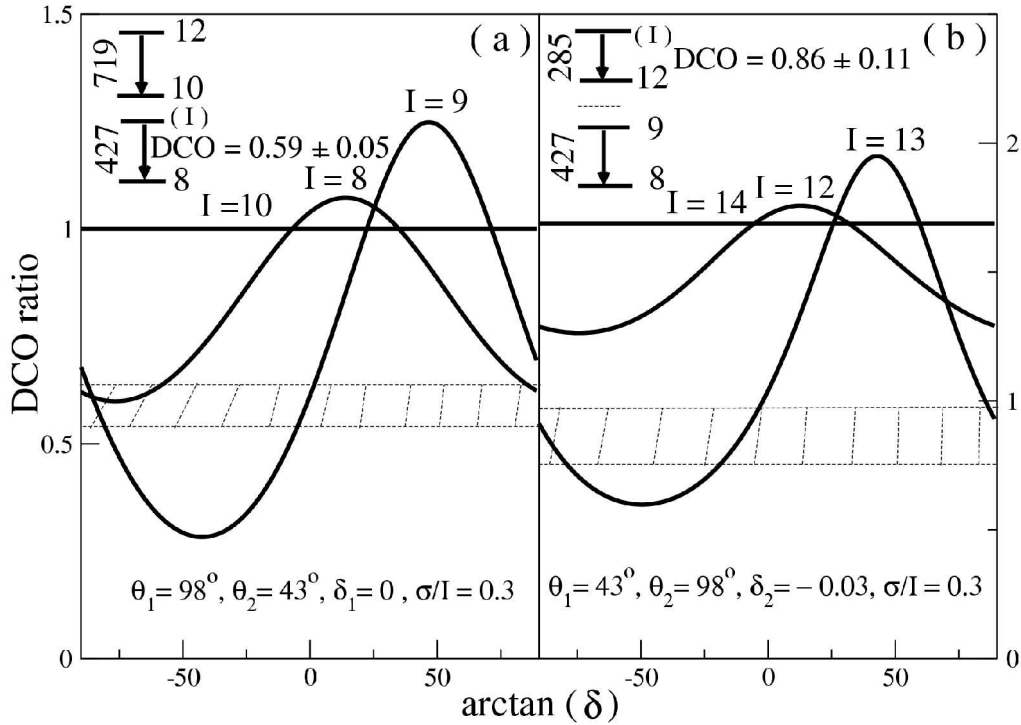


**Fig. 3 : DCO ratio for the transitions (a) 719 keV - 427 keV & (b) 427 keV- 285 keV**

We have constructed the level scheme for  $^{134}\text{La}$ , as placing the known transitions as well as the new transitions with energy values ( keV ), 116, 130, 188, 285, 320, 359, 375, 403, 533, 538, 547, 557, 570, 574, 603, 604, 617, 675, 680, 697, 705, 708, 840, 843, 1131, 1609 and 1971. The new transitions are shown as dotted lines in Fig. 1. Most of the new transitions belong to a band, not known from the earlier measurements [1,5,6]. Unfortunately, we were not able to add any new transition belonging to the chiral partner band. As a result, the uncertainty about its existence still persists.

## REFERENCES

53. R.A. Bark *et. Al.*, Nucl. Phys. A691 (2001) 577.
54. FREEDOM: a computer program procured from N.S.C., New Delhi, India.
55. D.C. Radford, Nucl. Instrum. Methods Phys. Res. Res. A 361 (1995) 297.
56. K.S. Krane *et.al.*, Nucl. Data Table A 11( 1973) 351.
57. U. Datta pramanik *et. al.*, Nucl. Phys. A637 (1998) 327.
58. P. Das, In proc. National Workshop on directions in Nuclear Structure Research at High Angular Momentum, Dept. of Physics, Univ. of Bombay (1994).

### 5.1.9 New measurement of astrophysical $S_{17}$ factor from $d(^7\text{Be}, ^8\text{B})n$ at $E_{\text{cm}}=4.4$ MeV

JJ Das<sup>10</sup>, V M Datar<sup>1</sup>, P Sugathan<sup>10</sup>, N Madhavan<sup>10</sup>, P V Madhusudhana Rao<sup>10</sup>,  
A Navin<sup>1</sup>, A Jhingan<sup>10</sup>, T Varughese<sup>10</sup>, S Nath<sup>10</sup>, A Ray<sup>2</sup>, S Barua<sup>3</sup>, R Singh<sup>4</sup>,  
S K Dhiman<sup>5</sup>, R Shyam<sup>6</sup>, R G Kulkarni<sup>7</sup>, A K sinha<sup>8</sup> and D L Shastri<sup>9</sup>

<sup>1</sup>Nuclear Physics Division, Bhabha Atomic Research Centre, Mumbai.

<sup>2</sup>Variable Energy Cyclotron Centre, Bidhan Nagar, Kolkata

<sup>3</sup>Department of Physics, Guwahati University, Jalukabari, Guwahati.

<sup>4</sup>Department of Physics and Astro-Physics, Delhi University, Delhi

<sup>5</sup>Department of Physics, Himachal Pradesh University, Shimla

<sup>6</sup>Saha Institute of Nuclear Physics, Kolkata, India

<sup>7</sup>Department of Phys. Saurashtra University, Rajkot, India

<sup>8</sup>Inter University Centre for DAE Facilities, Kolkata

<sup>9</sup>Department of Nuclear Physics, Andhra University, Visakhapatnam, India

<sup>10</sup>Nuclear Science Centre, New Delhi-110 067

The  $^7\text{Be}(p,\gamma)$  cross section at low energies has been of interest in nuclear astrophysics for more than three decades. This cross section also has a bearing on details of the solar neutrino flux measurements by the groups at SNO, SuperKamioka, Homestake and Gran Sasso (Gallex) [1]. There are several attempts to derive the  $S_{17}(0)$  factor using different methods. The results of these measurements lie within a band between 17 and 24 eVb. The errors in direct measurements have successively been reduced from various systematics. The need to reduce the error in the  $S_{17}(0)$  below 5% [2] has been addressed by the most recent direct  $^7\text{Be}(p,\gamma)$  measurements [3]. However these measurements do not all agree within the quoted errors. In the review [2], Adelberger has emphasised the importance of additional indirect determinations of  $S_{17}(0)$  which are sensitive to different systematic effects from those present in the direct cross-section measurements. One kind of indirect measurement uses the Coulomb breakup reaction [4]. The other technique uses the  $(^7\text{Be}, ^8\text{B})$  transfer reaction to extract the magnitude of the asymptotic radial wave function, characterized by the asymptotic normalisation coefficient(ANC), of the proton in  $^8\text{B}$  which is then used to calculate the  $^7\text{Be}(p,\gamma)$  cross section, and hence the  $S_{17}$  factor, at energies of astrophysical interest [5]. After initial work of Liu et. al. to estimate  $S_{17}$  using the  $^2\text{H}(^7\text{Be}, ^8\text{B})n$  reaction, this measurement was repeated using more sophisticated setup at MSU, RIKEN for more accurate results [6]. Though deuteron is possibly the simplest target for the ANC method to be reliably used, ambiguities regarding the choice of optical model parameters still persists resulting in substantial uncertainty in extracted  $S_{17}(0)$  from these measurements [7]. More recent experiments using heavier targets like  $^{10}\text{B}, ^{14}\text{N}$  with  $^7\text{Be}$  beam were done at Texas A&M institute and  $S_{17}(0)$  factor was extracted using ANC method but its value is lower [8].

In this report, we present the preliminary result of our experiment to extract  $S_{17}(0)$  using  $^2\text{H}(^7\text{Be}, ^8\text{B})n$  reaction at  $E_{\text{cm}} = 4.4$  MeV which is the lowest energy measurement attempted so far. The aim was to reduce both statistical and systematic error reported in

earlier measurements [6,8]. We faced added complexities arising out of lower energy and higher beam flux which were solved in few iterations apart from solving the difficulties associated with the RIB production and the development of the detection setup.

The  $^7\text{Be}$  beam was produced by operating the existing recoil mass separator in a novel optical mode [9] with added new hardware leading to a beam of much better quality and lower systematic errors. Special techniques were developed for reproducibility of beam trajectory required for angular distribution measurement in inverse kinematics using RIBs. In addition the OMP parameters in the entrance channel have been constrained through a separate elastic scattering measurement done at an identical CM energy.

The detector setup consisted of a MWPC counter followed by a Ta disc of 4 mm dia. along beam path downstream of the target primarily to stop  $^7\text{Be}$  particles without major loss of  $^8\text{B}$  particles. The disc was also made removable to get zero degree data under identical experimental condition. This reduced the  $^7\text{Be}$  flux in detector setup by more than 4 times. The Anode energy output pulse of MWPC was taken directly to an MCA for counting incident flux. Anode timing pulse was used with RF for eventwise monitoring of TOF of particles. Fig. 1 shows the TOF spectra, which immediately shows the purity of the beam.

To measure the response of the telescope detector setup in situ, the RMS was rotated to  $2^\circ$  and scattered  $^7\text{Li}$  and  $^{12}\text{C}$  ions selected with appropriate scaling of the fields of the spectrometer. This was crucial in choosing the  $\Delta E$ -E two dimensional gates in conjunction with simulation. Fig. 2 shows the observed spectra along with simulated gates.

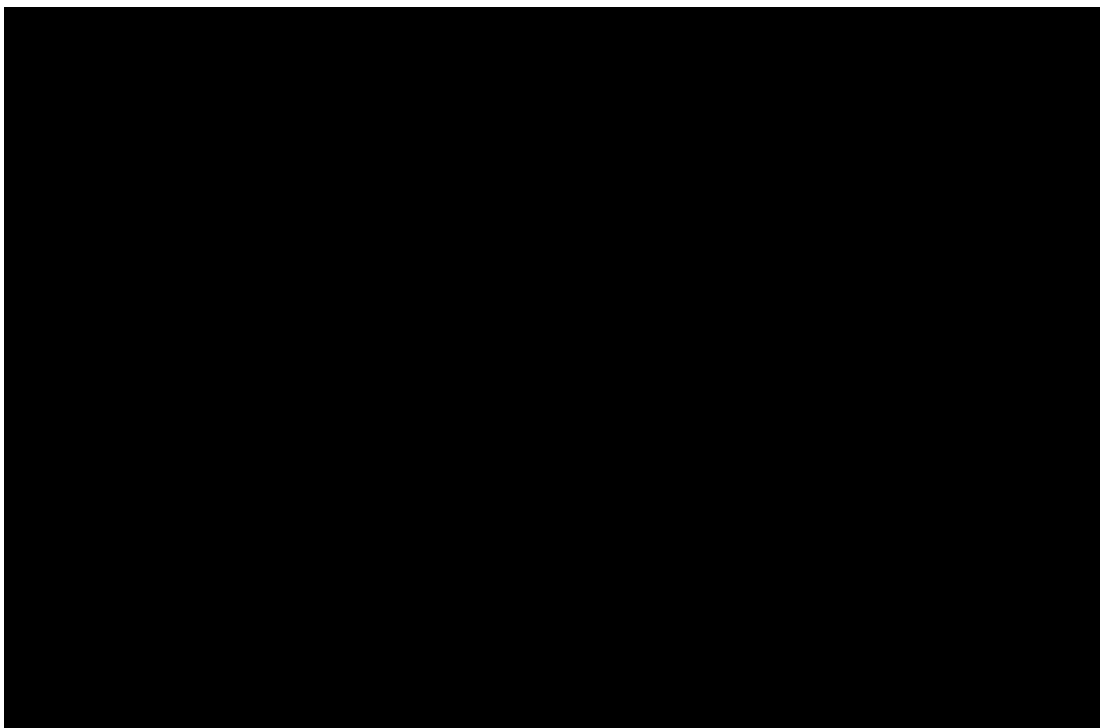


**Fig. 1 : Time of flight spectrum for detected particles**

**Fig. 2 : DE-E Calibration spectrum taken with  $\alpha$ ,  ${}^7\text{Li}$ ,  ${}^7\text{Be}$ ,  ${}^8\text{B}$  and  ${}^{12}\text{C}$  as shown by bands**

The data were sorted with suitable two dimensional gates on the  $\Delta\text{E-E}$ , pileup parameter and TOF. The projected X-Y two dimensional spectra of the  ${}^8\text{B}$  events in the Silicon detector were used to obtain the angular distribution in the laboratory system. The

non-linearity in the position response of the Si detector was determined using an alpha source and a precision mask placed directly on the detector. For determining the angular distribution a threshold of 1 MeV was used on the Si detector. The overall angular resolution was simulated taking into account the angular divergence of the beam, transverse beam profile, angular straggling in the target and gas and the angular resolution of the Si detector to be 0.9 degrees. Necessary corrections were made for the efficiencies of the TOF, pileup gates, transmission through wire mesh of detector setup. Dead time of the acquisition system was determined online. Fig. 3a & b shows the final mass spectra for CH<sub>2</sub> target and CD<sub>2</sub> target with similar flux. Fig. 4 shows the preliminary result of our experiment. Further theoretical work along with folding is in progress to restrict the choice of optical model parameters using the <sup>7</sup>Be+d-><sup>7</sup>Be+d measurement done using the same facility.

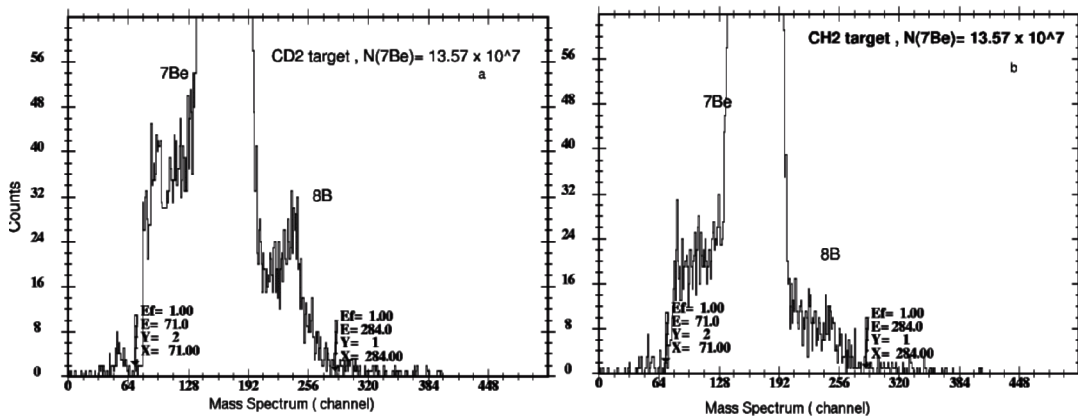


Fig. 3 : Mass spectra for (a) CH<sub>2</sub> target and (b) CD<sub>2</sub> target with similar flux

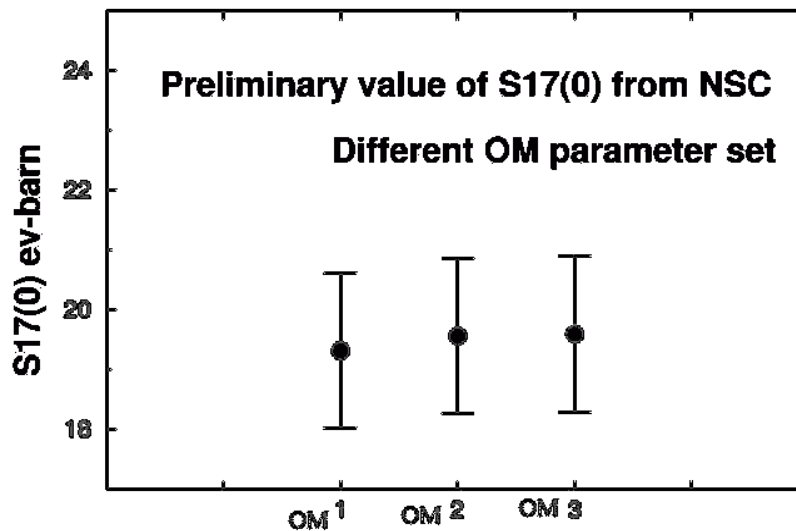


Fig. 4 : S<sub>17</sub>(0) factor extracted from the present data using different Optical model parameter set

## REFERENCES

59. J.N. Bahcall, Neutrino 2002.
60. E.G. Adelberger et al, Rev. Mod. Phys. **70**, 1265 (1998).
61. B.W. Phillipone et al, Phys. Rev. Lett. **50**, 412 (1983); Phys **C28**, 2222 (1983) ; F. Hammache et al, Phys. Rev. Lett. **80**, 928 (1998); M. Hass et al, Phys. Lett. **B462**, 237 (1999); A.R. Junghans et al, Phys.Rev. Lett. **88**, 041101 (2002); L.T. Baby et al, Los Alamos preprint archive, arXiv:nucl-ex/**0208005v3** (2002)
62. F. Streider et al, Nucl. Phys. **A696**, 219 (2001); T. Motobayashi et al, Phys. Rev. Lett. **73**, 2680 (1994); T. Kikuchi et al, Eur. Phys. J. **A3**, 213 (1998); B. Davids et al, Phys. Rev. Lett. **86**, 2750 (2001).
63. H.M. Xu et al, Phys. Rev. Lett. **73**, 2027 (1994).
64. W. Liu et al, Phys. Rev. Lett. **77**, 611 (1996); C Powell et. al. in Proc. of ENAM-98, pg no. 455 (AIP); M Ishiara et. al. RIKEN proposal to study  $d(^7\text{Be},^8\text{B})n$  ; D Beaumel et. al. ORSAY-RIKEN collaboration for measurement of  $s_{17}(0)$  through  $d(^7\text{Be},^8\text{B})n$  reaction at PRO-RIB-2001, in Indian Journal of Phys. 76S(I),145-147(2002).
65. Gagliardi et. al. Phys Rev. Lett 80,421 (1998); J.C. Fernandes, R. Crespo, F.M. Nunes and I.J. Thompson, Phys. Rev. **59**, 2865 (1999).
66. A. Azhari et al, Phys. Rev. Lett. **82**, 3960 (1999) ; A. Azhari et al, Phys. Rev. **C60** 055802 (1999); A. Azhari et al, Phys. Rev. **C63** 055803 (2001);
67. JJ Das et. al. Journal of Phys. **G 24**(1998)1371 and references there in ; JJ Das et. al. Indian J Phys. 76S(I)133-137(2002).

### 5.1.10 First measurement of Elastic scattering of the $d(^7\text{Be},^7\text{Be})d$ system at $E_{\text{CM}}=4.3$ MeV using kinematics coincidence

S. Barua<sup>1</sup>, J.J. Das<sup>4</sup>, A. Jhingan<sup>4</sup>, T. Varughese<sup>4</sup>, N. Madhavan<sup>4</sup>, P.V. Madhusudhana Rao<sup>4</sup>, B. Bhattacharya<sup>1</sup>, K. Kalita<sup>3</sup>, S. Verma<sup>3</sup>, P. Sugathan<sup>4</sup>, V.M. Datar<sup>2</sup>, A. Navin<sup>2</sup>, S. Nath<sup>4</sup>, R. Singh<sup>3</sup>, S.K. Datta<sup>4</sup> and K. Barua<sup>1</sup>

<sup>1</sup>Dept. of Physics Guwahati University, Guwahati, Assam-787014

<sup>2</sup>Nuclear Physics division, BARC, Mumbai

<sup>3</sup>Dept. of Physics and Astrophysics, Delhi University, Delhi-110007

<sup>4</sup>Nuclear Science Centre, New Delhi-110 067

Measurement of elastic scattering cross-section in the  $^7\text{Be}+d \rightarrow ^7\text{Be}+d$  has been a topic of considerable discussion following the extraction of  $S_{17}(0)$  by Xu. et. al using  $^7\text{Be}(d,n)^8\text{B}$  reaction [1,2]. It has been emphasized that it is impossible to chose a unique set of OM parameters if  $E_{\text{CM}} > 15$  MeV even if elastic scattering is measured [3], which has been also the conclusion of two recent experiments at NSCL and RIKEN-ORSAY collaboration [4]. However, theoretical calculation does predict that at a lower energy, elastic scattering data could reduce these ambiguities. In this report, we briefly mention the results of first such measurements.

Elastic scattering measurement with a compound target like  $\text{CD}_2$  is a difficult proposition with RIBs, as beam has a energy and angular spread. Apart from this low energy tail can also create additional problem. So we opted for the measurement in the kinematic coincidence mode of the detectors which can eliminate the effect of low energy tail as well the large elastic scattering of  $^7\text{Be}$  from the Carbon in  $\text{CD}_2$ .

The present experiment of measuring elastic angular distribution of  $^7\text{Be} + d$  has two purposes :

68. To get the elastic angular distribution of the same at this low energy to extract the optical model parameters which is required extract  $S_{17}(0)$  factor .
69. To test the kinematic mode of the detector system made to use in the  $^7\text{Be}+^7\text{Li}$  scattering experiment in kinematic co-incidence mode

The  $^7\text{Be}$  of  $E_{\text{lab}}=20.25$  MeV produced in the RIB facility [5] at NSC was incident on  $1.0$  mg/cm<sup>2</sup> thick  $\text{CD}_2$  target, kept at the second focal plane of HIRA, in order to measure the elastic scattering of  $^7\text{Be}+d \rightarrow ^7\text{Be}+d$  using kinematics coincidence. The details of the detector system is described elsewhere[6] . In this detector setup, the front annular detector and the back PSSD (2D) are in kinematic coincidence mode The nominal angular coverage of the first annular detector from the beam axis is from  $53^\circ$  to  $72^\circ$ . Actual angular acceptance spread gets broader ( $50^\circ - 73^\circ$ ) mostly caused by

70. by the finite width of the beam spot size  $\sim 3$  mm fwhm ( $\pm 2^\circ$ )
71. intrinsic angular spread of the beam ( $\pm 1^\circ$ )
72. angular straggling in the target .

As the kinematics is highly inverse, recoils focus into a small forward angle ( $< 16$  degree) and the forward branch is detected with complete efficiency except for the small masking by the stopper put in front of the 2D detector. Corresponding deuterons recoiling at backward direction in CM system (still forward in laboratory frame) are detected in the first annular detector. So for all the deuterons detected in the angular range of (50-73 degree) in lab has corresponding  $^7\text{Be}$  detected in the gas DE-Si(2D) telescope detector.

After the energy and position calibration of the detectors and the offset correction of the various ADCs, the extraction of the data became easier and cleaner with the imposition of kinematic coincidence condition. Fig. 1a-b show the cleaning up of the position spectrum of the  $^7\text{Be}$  on 2D without (a) and with (b) the kinematic coincidence condition.

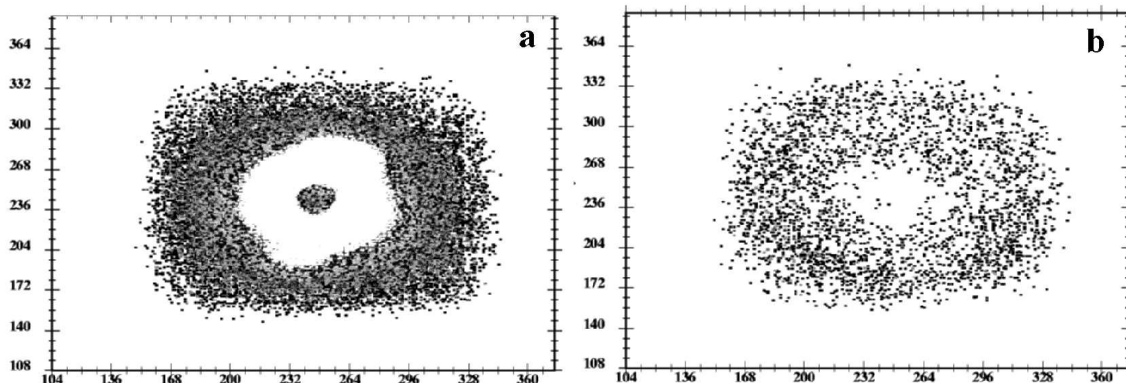


Fig. 1 : (a) Raw 2D position spectrum (b) 2D position spectrum with kin.coincidence

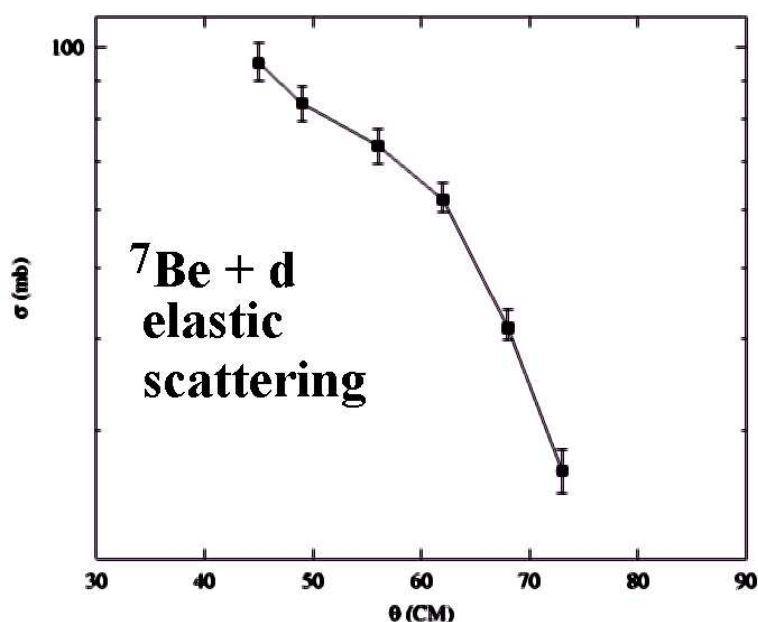


Fig. 2 : Angular distribution of  ${}^7\text{Be} + \text{d}$  elastic scattering

The data analysis is in progress and in the final stage now. Fig. 2 shows the preliminary angular distribution of  ${}^7\text{Be}$  extracted from the experimental data which will get considerably modified because of the intrinsic energy and angular spread of the beam and finite resolution of the detector and uncertainties related to target straggling and reproduction of beam axis. So, to compare theoretical results, an iterative approach need to be adopted where in theoretical results are folded with experimental folding function.

## REFERENCES

73. Liu et. al PRL 77(611) (1996)
74. CA Gagliardi et. al. PRL 80, 421(1998)
75. C Fernandez et. al. PRC 59,2865(1999)
76. D Beaumel et. al. Proc of PRO-RIB, IJP Vol. 85A,no 4 Pg 145.

77. J.J.Das et.al. J.Physics G,24(1998)1371  
78. A. Jhingan et.al DAE symposium, 2002.

### 5.1.11 Elastic Scattering of ${}^7\text{Be}+{}^7\text{Li}$ Experiment

S.Barua<sup>1</sup>, B.Bhattacharjee<sup>1</sup>, K.Baruah<sup>1</sup>, J.J.Das<sup>3</sup>, T.Varughese<sup>3</sup>, Akhil Jhingan<sup>3</sup>, N Madhavan<sup>3</sup>, P.Sugathan<sup>3</sup>, P.V.Madhusudhana Rao<sup>3</sup>, S.Nath<sup>3</sup>, S.K.Datta<sup>3</sup>, K.Kalita<sup>2</sup>, S.Verma<sup>2</sup> and R. Singh<sup>2</sup>

<sup>1</sup>Dept. of Physics, Gauhati University, Guwahati-781014

<sup>2</sup>Dept. of Physics and Astrophysics, Delhi University, Delhi-110007

<sup>3</sup>Nuclear Science Centre, New Delhi-110067

Experimental measurement in mirror nuclear Elastic scattering in the  ${}^7\text{Be} + {}^7\text{Li}$  system around barrier has become accessible at NSC with the production of  ${}^7\text{Be}$  RIB recently [1]. This measurement was attempted earlier at LANL [2] to verify the theory of resonant charge exchange process in mirror nuclei proposed by Vary and Nagarajan [3]. However, no definitive conclusions could be drawn from the experiment, mainly because of experimental limitations. This experiment is sought to be repeated here with the NSC facility under improved experimental setup [4]. However, as estimation of cross-section of such process is difficult because of lack of systematic experimental study. So, our main emphasis is on measuring the angular distribution of the elastic scattering, which would be new at this energy.

All the necessary hardware for the experiment has been designed, fabricated and tested and the experiment was performed using 20.25 MeV  ${}^7\text{Be}$  beam on enriched  ${}^7\text{Li}$  target. We mention below the details of development undertaken as well as preliminary results.

Let us first mention few difficulties we anticipated while planning this elastic scattering experiments using  ${}^7\text{Be}$  beam. Firstly the RIB, produced using in-flight technique, has intrinsic energy and angular spread caused by the production reaction and target thickness. These spreads are limited by the acceptance of the spectrometer as well as by slits/apertures at various places along the flight path of the ions. Narrowing down these slits very tightly to reduce spreads further is not possible as RIB intensity will fall. So a compromise is normally made between the required beam intensity and acceptable beam quality. Typically, we operate with  $\pm 30$  mrad angular and  $\pm 2.5\%$  energy spread @ 5-10 KHz flux. To compensate this low beam intensity, high efficiency, discriminative detector systems are required. Development of such a setup was our first major job.

Secondly, the energy spectrum of  ${}^7\text{Be}$  beam shows a low energy tail. This is caused by scattering of beam from the slit systems in the spectrometer. These scattered particles do not follow the mean ion optical trajectory and hence are not focused to a narrow spot and show up as tails in position spectra (beam halo). Typically, in an optimised settings, such events are  $\sim 1\%$ . Presence of these tails make elastic scattering

measurement quite difficult as actual scattering events at any given angle will get contaminated by these random events. One way to estimate this background is through subtraction technique, we decided to use "kinematic coincidence" technique.

A new and large area Annular detector setup was designed for this purpose. Inter-detector separation were minimised to the extent possible with the requirement of two body kinematics for coincidence so that both the particles would be detected simultaneously in either of the detectors. As particles originating from position or energy tail detected in one detector will not have any correlated counterpart on the other detector and will be eliminated automatically.

Another difficulty specific to this particular experiment arises from the hygroscopic and easily oxidizable nature of  ${}^7\text{Li}$  target. It quickly forms a compound coming in contact with air. So, elastic scattering from  ${}^7\text{Li}$  target would be contaminated by Rutherford scattering from higher  $Z$  elements. Thicker layer of contamination can drastically reduce the Kinematics coincidence efficiency as well. For this, a new target mechanism with magnetically coupled drive was developed for transferring of the target from the place of fabrication to the experimental site. It may be mentioned here that this is the first preparation of  ${}^7\text{Li}$  target here.

The details of the detector system is described elsewhere[4]. The front and the back annular detectors are in the kinematic coincidence mode for  ${}^7\text{Be}+{}^7\text{Li}$  elastic scattering. The first annular detector subtends angles from  $54^\circ - 70^\circ$  in the laboratory, detecting either the elastic recoils from the target or the back scattered projectile. The gas IC and the back annular/PSSD together work as a DE-E telescope. A Ta disc of 4 mm radius are put right on top of the PSSD along beam axis to stop the main beam from falling on the PSSD detector. The final angular range covered by the forward telescope are from  $3^\circ - 34^\circ$ .

Another important aspect in using annular detectors for measuring angular distribution is the axial alignment of the detector system. This was done mechanically through a specially fabricated alignment jig.

The in-vacuum target transfer system used to prepare pure  ${}^7\text{Li}$  target consists of a long magnetically coupled drive and tested to vacuum better than  $2.0 \times 10^{-6}$  torr. This drive is then mounted to X/Y movement assembly for alignment purpose. For alignment of target along beam axis first blank frames with thin  ${}^{12}\text{C}$  backing were aligned then the target of required thickness was evaporated. Special care was required to ensure that front annular detector is not damaged by any protrusion from target frame as it is very near to the target. The details of the target preparation is described elsewhere in this report [5].

20.25 MeV  ${}^7\text{Be}$  produced in the RIB facility at NSC was allowed to fall on the  $628 \mu\text{g}/\text{cm}^2$   ${}^7\text{Li}$  target which was made by evaporating the  ${}^7\text{Li}$  material on  $10 \mu\text{g}/\text{cm}^2$  Carbon backing, placed at the reaction chamber of HIRA. The electromagnetic spectrometer HIRA was tuned to make the beam exactly fall at the centre of the detector

system as well as on the target which is monitored from the position spectrum of the 2D detector. Fig. 1 shows the left/right and top/bottom half of the position counts of the 2D detector which almost fall in a horizontal straight line w.r.t. the run no. confirming the axial alignment of the detector system. All the amplifiers were gain matched using ORTAC-precision pulser. The alpha runs were also taken in between to see the consistency of the detector condition during the whole experiment. The alpha source was mounted on a shaft protruded from a MDC linear drive put in one port of the scattering chamber of HIRA focal plane and was put in the beam position when the alpha runs were taken and otherwise, pulled out and kept behind a mask. The pressure of the isobutene in the ionization chamber was maintained at  $95 \pm 0.5$  mbar, throughout the experiment.

The offset determination of the all ADC channels and gain matching of the energy signals and the position signals from various detectors was done with high precision ORTEC pulse generator and the thickness of the target was calculated from the  $dE/dX$  calculation of alpha energy loss in the target using  $^{241}\text{Am}$  source. The energy calibration of each detector energy and the position calibration of the same was done with alpha source and also with the beam. Now constructing a software gain matched  $E1+E2+E3$  ( $E1,2,3$ , total detected energy from an event,  $E1 = E_{\text{front annular}}$ ,  $E2 = E_{\text{IC}}$ ,  $E3 = E_{\text{back annular}}$ ) spectrum with the kinematics condition  $E1 > 100\text{KeV}$ , the total detected energy was being cleared up. In the  $E3-E2$  spectrum, now this cleared up energy condition was put which cleared the  $E3-E2$  spectrum. Further condition of TOF has cleared this spectrum from noise and other external source.

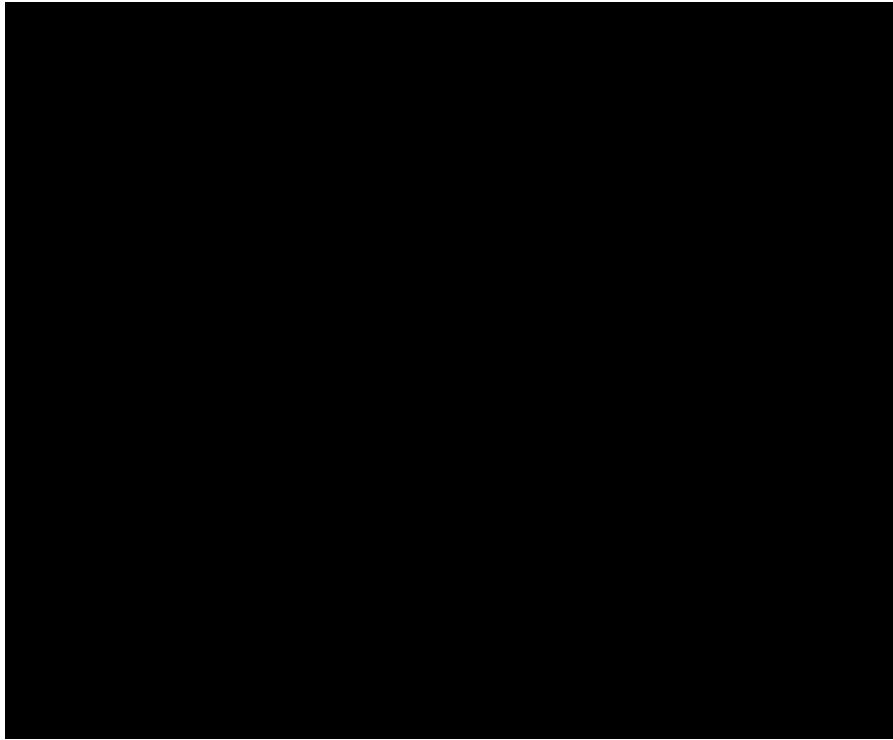


**Fig. 1 : Alignment varification of the detector system**

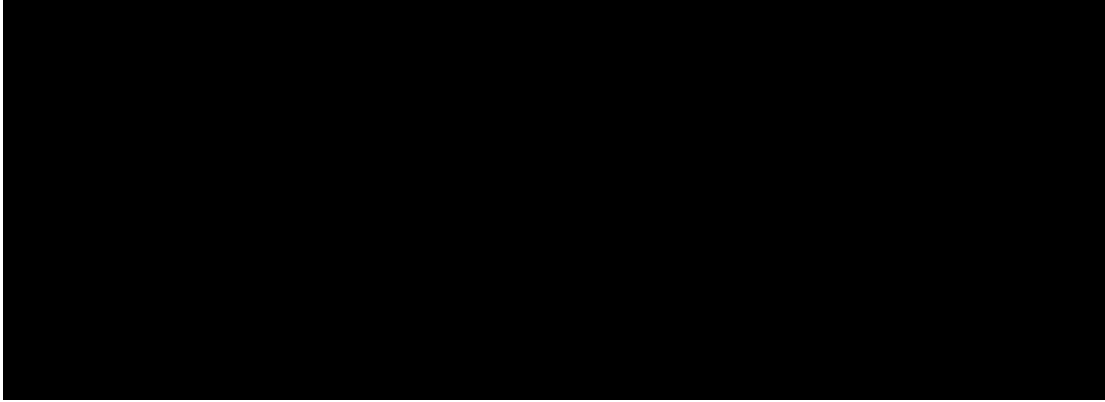


**Fig. 2 : The kinematics coincidence gated E123 spectrum (left) gets further cleaned up with the  $^7\text{Be}$  gate on it (right)**

Two banana gates were made on the two bands corresponding to  $^7\text{Be}$  and  $^7\text{Li}$ , from the E3-E2 ( E123 and TOF gated) spectrum. When this gate was put on E123 and T23, along with the kinematics coincidence condition, the counts were coming at the expected regions (Fig. 2), but a good peaked spectrum was not formed due to very low count rate. The analysis for this system is in progress.

## REFERENCES

79. J.J.Das et.al.,Journal of Phys.G,24(1998)1371
80. R.N.Boyd et.al. Proc. Of first Intl. Conf. On RIB,(1089),311
81. A.M.Nagarajan and J.P.Vary, Physical Rev.C,42,1(1991)281
82. A.Jhingan et.al. Proc. DAE symp. 2002
83. S.Barua et.al. Proc. DAE symp.2002

### 5.1.12 Change of $^7\text{Be}$ decay rate in $\text{C}_{60}$ fullerene: A new tool for studying atomic cluster

P. Das<sup>1</sup>, A. Ray<sup>1</sup>, S. K. Saha<sup>2</sup>, S. K. Das<sup>2</sup>, A. Mookerjee<sup>3</sup>, J.J. Das<sup>5</sup>, P. Sugathan<sup>5</sup>, N. Madhavan<sup>5</sup>, P.V. Madhusudhana Rao<sup>4,5</sup>, T. Varughese<sup>5</sup>, A. Jhingan<sup>5</sup> and S. Nath<sup>5</sup>

<sup>1</sup>Variable Energy Cyclotron Centre, 1/AF, Bidhannagar, Kolkata - 700064

<sup>2</sup>Radiochemistry Division, Variable Energy Cyclotron Centre, 1/AF, Bidhannagar, Kolkata - 700064

<sup>3</sup>S.N. Bose National Centre for Basic Sciences, 3/JD, Bidhannagar, Kolkata - 700091

<sup>4</sup>Department of Nuclear Physics, Andhra University, Visakhapatnam - 530003

<sup>5</sup>Nuclear Science Centre, New Delhi-110067

The effect of host medium on half-life of implanted  $^7\text{Be}$  is a topic of current interest and has contributed to many fields such as the development of solar model, test of weak interaction theory, condensed matter and atomic physics.  $^7\text{Be}$  is the lightest nucleus that decays by orbital electron capture and so its decay rate is most susceptible to the surrounding environment. Recent studies using nuclear implantation technique show that the presence of surrounding host atoms usually changes the half-life of  $^7\text{Be}$  by a small amount [1,2,3] but the L/K capture ratio of  $^7\text{Be}$  by a rather significant amount [4,5].

The change of  $^7\text{Be}$  decay rate in an atomic cluster such as  $\text{C}_{60}$  fullerene could be used as a tool to study about the ionization of  $^7\text{Be}$  in  $\text{C}_{60}$  fullerene and the formation of endohedral fullerene compound which has recently attracted much attention because of its interesting physical and chemical properties. It is already well-known [6,7,8] that different types of metal atoms(Be, Kr, Xe etc.) can be inserted into  $\text{C}_{60}$  fullerene cage forming endohedral compound by nuclear implantation technique. An interesting question is to know about the charge of the implanted ion and equilibrium geometry of the endohedral and exohedral fullerene complex.

Several theoretical studies [9,10] have been done regarding the charge of the implanted ion for both endohedral and exohedral fullerene complexes and the equilibrium geometry of the endohedral fullerene compound, but there are discrepancies among them even regarding the basic question whether  $^7\text{Be}$  implanted in fullerene  $\text{C}_{60}$  should lose most of its 2s electrons or approximately preserve its atomic electronic configuration. Aree et al. [9] studied endohedral  $\text{Li@C}_{60}$  complex using ab initio Hartree-Fock calculations and found that Li atom should almost lose its 2s electron when it is placed within  $1 \text{ \AA}$  from the center of fullerene cage. On the other hand, Lu et al. [10] found from their density functional calculation that for endohedral  $\text{Be@C}_{60}$  complex, Be atom should approximately preserve its 2s electrons when placed at the center of fullerene  $\text{C}_{60}$  cage, although the electron affinity of Be is almost zero whereas that of Li is  $=0.62 \text{ eV}$  [11]. So it is important to address these questions experimentally.

The half-life of  $^7\text{Be}$  implanted in fullerene  $\text{C}_{60}$  should show measurable change depending on whether  $^7\text{Be}$  loses most of its 2s electrons or retains them. So the change of half-life of  $^7\text{Be}$  in  $\text{C}_{60}$  fullerene compared to that in another well understood material could be used as a tool to learn about the ionization of  $^7\text{Be}$  in fullerene. We can also learn from such study about the equilibrium configuration and the probability of the formation of endohedral  $^7\text{Be@C}_{60}$  compound.

In this work, we have measured the difference of half-lives of  $^7\text{Be}$  implanted in gold (Au) and fullerene ( $\text{C}_{60}$ ). A  $25\mu\text{m}$  thick gold(Au) foil and a  $500\mu\text{m}$  thick fullerene( $\text{C}_{60}$ ) pellet were bombarded by a  $18 \text{ MeV}$   $^7\text{Be}$  beam from Nuclear Science Center, New Delhi, India. The ranges of  $18 \text{ MeV}$   $^7\text{Be}$  in Au and  $\text{C}_{60}$  are only  $12 \mu\text{m}$  and  $40 \mu\text{m}$  respectively. The intensity of the  $^7\text{Be}$  beam was about  $40,000$  particles/sec and the duration of the irradiation 24 hours for each sample. In order to obtain a  $18 \text{ MeV}$   $^7\text{Be}$  beam, a liquid nitrogen cooled hydrogen gas cell at one atmospheric pressure was bombarded with a  $15 \text{ pA}$   $21 \text{ MeV}$   $^7\text{Li}$  beam obtained from the Pelletron

machine of Nuclear Science Center, New Delhi, India. The  ${}^7\text{Be}$  nuclei produced by the reaction  $p({}^7\text{Li}, {}^7\text{Be})n$  at  $0^\circ$  were separated from the primary  ${}^7\text{Li}$  beam by using a recoil mass spectrometer called Heavy Ion Reaction Analyzer (HIRA) [12] operated in a suitable ion optical mode [13]. Primary  ${}^7\text{Li}$  beam particles were rejected by a slit system installed at the intermediate focal plane of the spectrometer. The primary beam rejection factor was about  $10^{10}$  and the purity of the separated  ${}^7\text{Be}$  beam was better than 99%. The advantage of using a high purity  ${}^7\text{Be}$  beam for implantation is to minimize the radiation damage of the sample and avoid production of unwanted radioactivity.

The  ${}^7\text{Be}$  implanted samples were brought to Variable Energy Cyclotron Center, Kolkata, India for off-line counting. Following electron capture, a  ${}^7\text{Be}$  nucleus has a 10.4% probability [14] of populating the first excited state of  ${}^7\text{Li}$  which decays subsequently to its ground state emitting a 478-keV  $\gamma$ -ray photon. Two HPGe detectors (detector-1 and detector-2) having efficiency  $\approx 30\%$  were used to count the samples ( ${}^7\text{Be}$  in Au and fullerene). A standard  ${}^{133}\text{Ba}$  source was placed in front of each HPGe detector and counted along with  ${}^7\text{Be}$  sources. The detectors were well shielded by lead bricks to avoid any cross-talk between them and also to reduce the background level.

A typical  $\gamma$ -ray spectrum (for  ${}^7\text{Be}$  in  $\text{C}_{60}$  fullerene) as recorded by detector-1 is shown in Fig. 1. Apart from 478 keV line coming from the decay of  ${}^7\text{Be}$  and other lines from  ${}^{133}\text{Ba}$ , we also see standard background lines such as 239 keV, 511 keV, 583 keV, 609 keV, 727 keV, 911 keV lines, but there was no other contaminant. The  $\gamma$ -ray spectrum of  ${}^7\text{Be}$  in Au also looks very similar to Fig. 1.

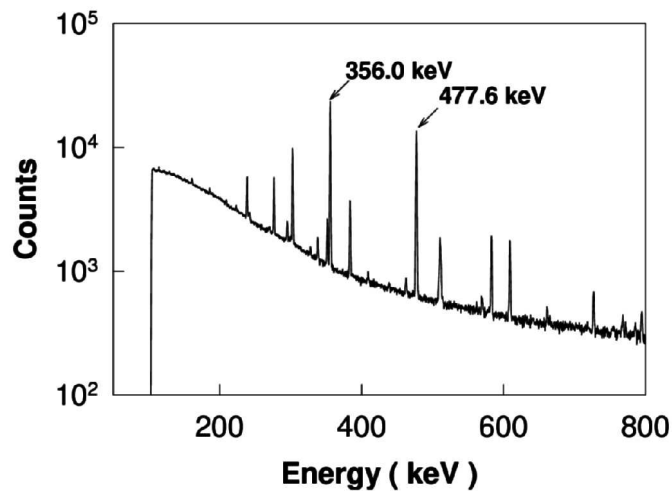


**Fig. 1 :  $\gamma$ -ray spectrum from the decay of  ${}^7\text{Be}$  implanted in  $\text{C}_{60}$  fullerene**

The count rate of 478 keV line was about 1 count per sec at the beginning of the run. Both the HPGe detectors were started at the same time, data was accumulated for 24 hours, stored in a computer and the spectra were cleared and the counting restarted.

After counting for at least a week, the positions of the samples were interchanged and counted again. This was done to take care of any systematic error. The counting was continued for about 6 months.

From each day's spectra, we determined the counts under 478 keV line ( $N_\gamma(478)$ ) and 356 keV line ( $N_\gamma(356)$ ) coming from  ${}^7\text{Be}$  and  ${}^{133}\text{Ba}$  respectively. The ratio  $N_\gamma(478)/N_\gamma(356)$  should be independent of computer dead time and any other systematic errors and it was monitored with time. In Fig. 2, we show plots of this ratio versus time and the corresponding exponential fits for (a)  ${}^7\text{Be}$  in Au and (b)  ${}^7\text{Be}$  in fullerene for detector-1. We also have similar data taken by detector-2 for  ${}^7\text{Be}$  in Au and fullerene along with the corresponding exponential fits. Taking weighted average of the results from detector-1 and detector-2, we finally obtain the percentage difference between the decay rates of  ${}^7\text{Be}$  in gold and fullerene to be  $[\lambda(\text{Au})-\lambda(\text{C}_{60})]/\lambda(\text{Au}) = (0.079 \pm 0.221)\%$ .

In a fullerene( $\text{C}_{60}$ ) lattice, sixty carbon atoms form a spherical shell or cage and then these spherical  $\text{C}_{60}$  cages are arranged in a face centered cubic lattice. The electron affinities of a fullerene molecule( $\text{C}_{60}$ ) and gold atom are about equal (2.6 eV [15] and 2.3 eV [11] respectively). Moreover both gold and fullerene have face-centered cubic (FCC) lattice structure. So the average number of 2s electrons of  ${}^7\text{Be}$  in Au and fullerene is expected to be similar. Hence the half-life of  ${}^7\text{Be}$  is qualitatively expected to be similar in fullerene and gold as we find experimentally. However, these results still do not give any direct evidence whether  ${}^7\text{Be}$  in Au or fullerene loses most of its 2s electrons.

Recently L/K electron capture ratio of  ${}^7\text{Be}$  implanted in mercury telluride (HgTe) was measured by Voytas et al. [4] and found to be less than half of the expected L/K capture ratio of a neutral free  ${}^7\text{Be}$  atom. This result shows that  ${}^7\text{Be}$  atom certainly loses on the average about half of its 2s electrons when  ${}^7\text{Be}$  is implanted in HgTe. This result was quantitatively understood using LMTO calculations [5] and gave us confidence in our LMTO method of calculation. Since the electron affinity [11] of Au is expected to be higher than that of HgTe, so  ${}^7\text{Be}$  in Au should lose a higher fraction of its 2s electrons compared to that of  ${}^7\text{Be}$  in HgTe. According to our earlier LMTO calculations [2], the average number of 2s electrons of implanted  ${}^7\text{Be}$  in Au is 0.416. So using Hartree's results [16], we conclude from our measured difference of half-lives of  ${}^7\text{Be}$  in Au and fullerene  $\text{C}_{60}$  that the average number of 2s electrons of  ${}^7\text{Be}$  in fullerene should be  $0.368 \pm 0.133$ .

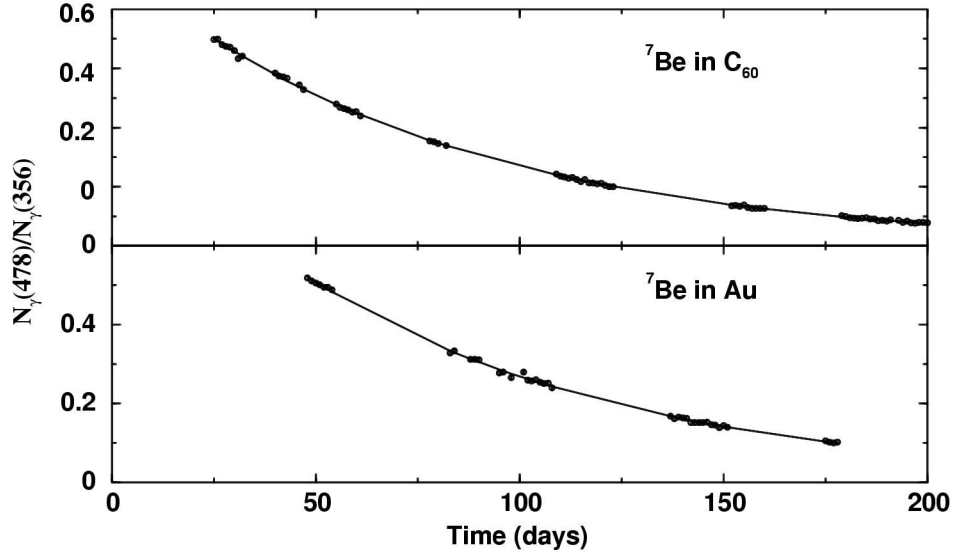


**Fig. 2 :  $N_{\gamma}(478)/N_{\gamma}(356)$  versus time for (a)  ${}^7\text{Be}$  in Au and (b)  ${}^7\text{Be}$  in Fullerene as measured by detector-1. Exponential fits are also shown**

We have done linear muffin-tin orbital (LMTO) method calculations [2,5,17] to determine the average number of 2s electrons of  ${}^7\text{Be}$  when  ${}^7\text{Be}$  is placed in different empty sites of fullerene  $\text{C}_{60}$  lattice. A fullerene molecule is constructed with 60 carbon atoms placed on a sphere of radius  $3.54 \text{ \AA}$ . These fullerene  $\text{C}_{60}$  molecules are arranged in a face-centered cubic structure with  $14.17 \text{ \AA}$  lattice constant. Using LMTO code [2,17], the available empty space in fullerene  $\text{C}_{60}$  lattice has been filled up with empty spheres to form a close packed system and the empty site locations are identified [18]. The calculations indicate that when  ${}^7\text{Be}$  is exactly at the center of fullerene  $\text{C}_{60}$  cage, then the its average number of 2s electrons will be between 0.000 to 0.019 and when it is exactly at the center of fullerene lattice, then the corresponding number should be between 1.58 to 2.00.

Our experimental result on the decay rate of  ${}^7\text{Be}$  in fullerene supports the physically plausible picture of  ${}^7\text{Be}$  occupying equilibrium positions at the center of  $\text{C}_{60}$  cage and fullerene lattice according to phase space. Considering the uncertainties of our measured difference of decay rates of  ${}^7\text{Be}$  in Au and  $\text{C}_{60}$  as well as the uncertainty of the calculated number of 2s electrons of  ${}^7\text{Be}$  at octahedral site, we estimate that the probability of the formation of endohedral  ${}^7\text{Be}@\text{C}_{60}$  is  $78 \pm 10\%$ . So we find that a very significant fraction of Be atoms can be put inside the fullerene  $\text{C}_{60}$  cage by nuclear implantation technique. This method should be, in general, very effective to produce any other type of endohedral metallofullerene and to study the equilibrium geometry of endohedral atomic cluster with beryllium.

In conclusion we find that the observed change of half-life of  ${}^7\text{Be}$  implanted in fullerene and gold is quantitatively well understood in terms of LMTO method [17] and Hartree's calculations [16] assuming that  ${}^7\text{Be}$  goes to equilibrium positions at the center of the fullerene  $\text{C}_{60}$  cage and lattice (octahedral site).  ${}^7\text{Be}$  should essentially lose all its 2s

electrons at the center of C<sub>60</sub> cage. On the other hand for exohedral case, when <sup>7</sup>Be is at the octahedral site, it should keep most of its 2s electrons. We also find that nuclear implantation technique is a very efficient method for the production of endohedral metallofullerene.

We acknowledge discussion with R. Vandenbosch (University of Washington, USA), Ove Jepsen (Max Planck Institute, Stuttgart, Germany) and J. Lu (Peking University, Beijing, China).

## REFERENCES

84. F. Lagoutine, J. L. Legrani and C. Bac, International Journal of Applied Radiation and Isotopes **25**, 131 (1975).
85. A. Ray, P. Das, S. K. Saha, S. K. Das, B. Sethi, A. Mookerjee, C. Basu Chaudhuri, G. Pari, Phys. Lett. B **455**, 69 (1999).
86. E. B. Norman et al., Phys. Lett. B **519**, 15 (2001).
87. P. A. Voytas et al., Phys. Rev. Lett. **88**, 012501 (2002).
88. A. Ray, P. Das, S. K. Saha, S. K. Das, A. Mookerjee, Phys. Rev. **C66**, 012501(R) (2002).
89. T. Ohtsuki et al., Phys. Rev. Lett. **77**, 3522 (1996).
90. T. Ohtsuki et al., Phys. Rev. Lett. **81**, 967 (1998).
91. T. Braun, H. Rausch, Journal of Radioanalytical and Nuclear Chemistry, **243**, 27 (1999).
92. Thammarat Aree, Teerakiat Kerdcharoen and Supot Hannongbua, Chem. Phys. Lett. **285**, 221 (1998).
93. Jing Lu, Yunsong Zhou, Xinwei Zhang and Xiangeng Zhao, Chem. Phys. Lett., **352**, 8 (2002).
94. CRC Handbook of Chemistry and Physics, by R. David (Ed.), Lide, 1994-95.
95. A. K. Sinha et al. Nucl. Instr. and Meth. **A339**, 543 (1994).
96. J. J. Das et al., Journal of Phys. G **24**, 1371 (1998).
97. Table of Isotopes, 8th Edition, by R. B. Firestone and V. S. Shirley (Ed.), John Wiley and Sons, Inc., 1999.
98. Lai Sheng Wang et al. Chem. Phys. Lett. **182**, 5 (1991).
99. D. R. Hartree and W. Hartree, Proc. Roy. Soc. (London) **A 150**, 9 (1935).
100. O. K. Andersen, O. Jepsen and D. Glotzl, Highlights of Condensed Matter Theory (North Holland, New York), 1985; O. K. Andersen, Z. Pawlowska and O. Jepsen, Phys. Rev. B **34**, 5253 (1986).
101. S. Satpathy, V. P. Antropov, O. K. Andersen, O. Jepsen, O. Gunnarsson and A. I. Liechtenstein, Phys. Rev. B **46**, 1773 (1992).
102. J. Hernandez-Rojas, J. Breton, J. M. Gomez Llorente, Chem. Phys. Lett. **235**, 160 (1995).
103. D. S. Bethune, R. D. Johnson, J. R. Salem, M. S. deVries, C. S. Yannoni, Nature **366**, 123 (1993).

### 5.1.13 Neutron evaporation as a probe of entrance channel effects in the heavy ion induced fusion reactions

Ajay Kumar<sup>1</sup>, A. Kumar<sup>1</sup>, G. Singh<sup>1</sup>, Hardev Singh<sup>1</sup>, R.P. Singh<sup>2</sup>, Rakesh Kumar<sup>2</sup>, K.S. Golda<sup>2</sup>, S.K. Datta<sup>2</sup> and I.M. Govil<sup>1</sup>

<sup>1</sup>Department of Physics, Panjab University, Chandigarh-160014, India

<sup>2</sup>Nuclear Science Centre, New Delhi-110067

Neutron spectra from the fusion reactions  $^{12}\text{C}+^{64}\text{Zn}$  at 85 MeV and  $^{31}\text{P}+^{45}\text{Sc}$  at 112 and 120 MeV have been measured in two series of complementary experiments using the time of flight technique. The energies are selected so that both of these systems lead to the compound nucleus  $^{76}\text{Kr}^*$  with the same value of the angular momentum and the excitation energy. The spectra from the asymmetric reaction  $^{12}\text{C}+^{64}\text{Zn}$  are found to be consistent with the predictions of the statistical model calculations using rotating liquid drop model values of the moment of inertia and the transmission coefficients for the spherical nuclei in the inverse absorption channel [Fig. 1]. However, the experimental spectra in the case of the symmetric reaction  $^{31}\text{P}+^{45}\text{Sc}$  show deviations at higher energies from the normal statistical model calculations. This indicates the effect of the entrance channel on the dynamics of the neutron evaporation of the compound system. The effective level density parameter  $a$  is found to be smaller, indicating the evaporation at a higher temperature, for the same compound nucleus formed in the case of the symmetric system as compared to the asymmetric system.

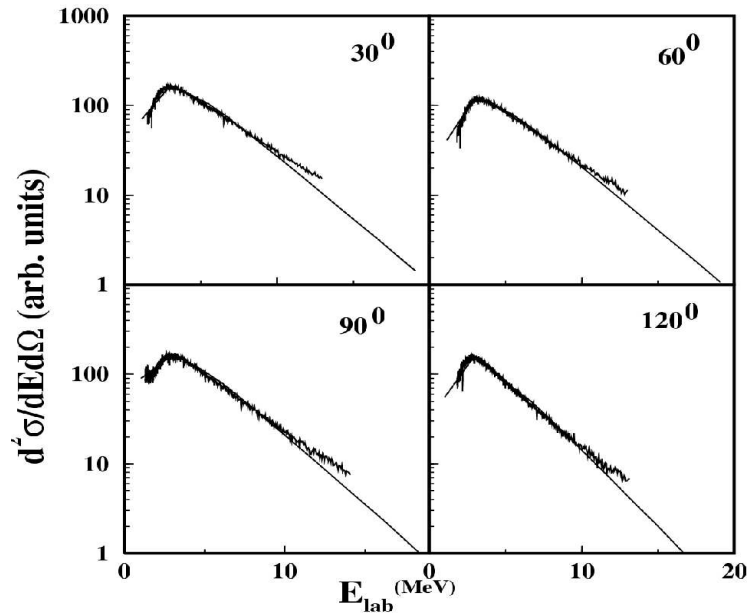


**Fig. 1 :** Comparison of the experimental neutron spectra (circles) with statistical model (solid line) using  $r_0 = 1.25$  and  $a = A/8$  for the asymmetric reaction  $^{12}\text{C}+^{64}\text{Zn}$  with  $I_{\text{max}} = 39\hbar$  and  $E^* = 75$  MeV at  $E_{\text{lab}} = 85$  MeV

### 5.1.14 Energy and Time Response of Stilbene Scintillator for Proton Energy Ranging from 5-25 MEV

A.Arulchakkaravarthi<sup>1</sup>, Rakeshkumar<sup>5</sup>, S.Muralithar<sup>5</sup>, R.P.Singh<sup>5</sup>, K.S.Golda<sup>5</sup>, Hardev Singh<sup>3</sup>, Asiti Sharma<sup>5</sup>, K.Sivaji<sup>4</sup>, P.Santhanaraghavan<sup>2</sup>, T.Nagarajan<sup>1</sup>, P.Ramasamy<sup>1</sup>, R.K.Bhowmik<sup>5</sup>

<sup>1</sup>Crystal Growth Centre, Anna University, Chennai-25

<sup>2</sup>Madras Institute of Technology, Anna University, Chennai

<sup>3</sup>Punjab University, Chandigarh

<sup>4</sup>Materials Science Center, Department of Nuclear Physics University of University, Chennai-25

<sup>5</sup>Nuclear Science Center, New Delhi-110 067

Pulse shape analysis in the crossing mode is used to discriminate radiations with different decay times in stilbene scintillator. In stilbene scintillator, the decay time of the fast component depends upon the nature of radiation and hence specific energy loss  $dE/dx$  in the detector. It is essential that the characteristics of the scintillation counter be accurately known in order that the observed pulse height distribution may be satisfactorily related to the scintillation intensity. Time and energy response of stilbene with respect to different energies of variety of particles has been studied extensively by many researchers in the past. Recent theoretical predictions by Papadopoulos [1,2] on rise time shift on stilbene scintillator concludes that for proton energies larger than 8.9 MeV the rise time shift increases suddenly and the energy response of stilbene to protons is non linear. In the present experiment the shift in the rise time of scintillation emission for different energy of protons has been recorded using pulse shape discriminator (CANBERRA 6120). Fast photomultiplier (Philips XP2020) having transit time spread (TTS) of 230ps has been used. Good calibration for energy as well as time with different bias voltages has been carried out and it was observed that -1600 V was optimum for present experiments. Amplifier with ADC has been used for recording the energy spectrum of protons ranging from 5 MeV to 25 MeV. It is observed that the rise time shifts towards lower channel side as the energy of proton increases. The energy response of stilbene for proton in the energy range from 5 to 25 MeV in the present experiment is linear. The results are not in agreement with the theoretical predictions of Papadopoulos [1,2].

### REFERENCES

104. L.Papadopoulos, Nucl. Inst. Methods, A Vol.434, (1999) 337.
105. L. Papadopoulos, Nuclear Instruments and Methods in Physics Research A Vol. 401 (1997) 322.

### 5.1.15 Mass Distribution Study of spherical nuclei

T.K.Ghosh<sup>1</sup>, N. Majumdar<sup>1</sup>, S. Pal<sup>1</sup>, S.Chattopadhyay<sup>1</sup>, P. Bhattacharya<sup>1</sup>, D.C. Biswas<sup>2</sup>, A. Saxena<sup>2</sup>, P.K. Sahu<sup>2</sup>, K.S. Golda<sup>3</sup> and S.K. Datta<sup>3</sup>

<sup>1</sup>Saha Institute of Nuclear Physics, 1/AF Bidhanagar, Kolkata-700 064

<sup>2</sup>Nuclear Physics Division, BARC, Anushaktinagar, Mumbai-400 085

<sup>3</sup>Nuclear Science Center, New Delhi-110 067

The signature of non-compound fission channel is reflected in the fragment mass distribution due to the incomplete equilibration in mass degree of freedom. The mass distribution for the systems  $^{16}\text{O} + ^{209}\text{Bi}$ ,  $^{19}\text{F} + ^{209}\text{Bi}$  has been studied at energies near and below the Coulomb barrier in order to understand the fission dynamics in case of spherical target. The experiments were carried out in the General Purpose Scattering Chamber (GPSC) at Nuclear Science Centre Pelletron, New Delhi, using pulsed beam. The beam resolution was found  $\sim 1.5$  ns. Two MWPCs (24 cm x 10 cm), developed at SINP, were kept at folding angle to catch the complementary fission fragments (FF). Timing, X-Y positions and energy loss of the FF in the detectors were collected in list mode. The fragment masses were determined from the time difference between the MWPC signals. The mass resolution of the set-ups were found to be  $\sim 4$  amu. The measured mass distributions for the systems were found to be symmetric in shape peaking around  $A_{\text{CN}}/2$ . However the variance of the mass distributions for the system  $^{16}\text{O} + ^{209}\text{Bi}$  was found to be nearly flat as a function of incident energy showing a barrier effect with a drop near the barrier and a consequent sharp rise.

### 5.1.16 Fission Fragment Anisotropies In The $^{12,13}\text{C} + ^{235}\text{U}$ System at Near and Sub Barrier Energies

B.P. Ajith Kumar<sup>6</sup>, K.M. Varier<sup>5</sup>, A..K. Sinha<sup>1</sup>, S.K. Datta<sup>6</sup>, N. Madhavan<sup>6</sup>, P. Sugathan<sup>6</sup>, A. Jhingan<sup>6</sup>, Subir Nath<sup>6</sup>, P. Barua<sup>6</sup>, P.V. Madhusudhana Rao<sup>6</sup>, S. Kailas<sup>2</sup>, B. Krishnarajulu<sup>3</sup> and Raghuvir Singh<sup>4</sup>

<sup>1</sup>IUC-DAEF, Calcutta Centre, Bidhan Nagar, Kolkata – 700009

<sup>2</sup>Nuclear Physics Division, BARC, Trombay, Mumbai – 400 085

<sup>3</sup>Department of Physics, Osmania University, Hyderabad – 500 007

<sup>4</sup>Department of Physics, University of Delhi, Delhi

<sup>5</sup>Department of Physics, University of Calicut

<sup>6</sup>Nuclear Science Centre, New Delhi – 110067

It is well known that heavy ion induced fission on actinide nuclei shows anomalous fragment anisotropies at sub and near barrier regions over that predicted by the standard fission theory [1]. At above barrier energies, pre-equilibrium fission [2] is thought to be a probable cause of this anomalous behaviour and explanation in terms of critical mass asymmetry parameter (Businaro-Gallone) and entrance channel dependence

has been attempted. At sub barrier energies target deformation [3] has also been found to play a strong role and explanation in terms of quasifission model has been tried. More recently ground state spin seem to influence the measured anisotropy to a greater extent at sub barrier energies [4].

The present measurements have been carried out using 66 – 80 MeV  $^{12,13}\text{C}$  beams delivered by the 16UD Pelletron accelerator at the Nuclear Science Centre, New Delhi. The target used was  $^{232}\text{Th}$  with a thickness of  $\sim 200 \mu\text{g}/\text{cm}^2$ . The fission fragments, at laboratory angles between  $80^\circ - 160^\circ$  on the same side of the U target, were detected by a  $\Delta E-E$  telescope. The telescope consisted of a Silicon  $\Delta E$  detector, backed a silicon E detector. Two Si monitor detectors were placed at  $\pm 10^\circ$  with respect to the incident beam. These were used for incident beam monitoring. The entire set up was inside the General Purpose Scattering Chamber (GPSC) installed on one of the beam lines of the accelerator. The detector signals were amplified and fed to a CAMAC ADC, triggered by the strobe signal derived from the E output. Event-wise data were stored on to disk using the software FREEDOM [5] developed at the Nuclear Science Centre. The online data were sorted and analyzed by the offline option of the software.

In a typical 2D plot of the out puts of the telescopes the fission fragments appear on the top left of the plot, well separated from the elastically and in-elastically scattered projectiles and other lighter reaction products. This identification has been confirmed by an offline measurement with the target replaced by a spontaneous fission source ( $^{252}\text{Cf}$ ).

The angular distributions of the fission fragments were extracted from the raw data. Detailed analysis is in progress.

## REFERENCES

106. B.B.Back et. Al., Phys. Rev. C53 (1996) 1734
107. V.S.Ramamurthy et al., Phys. Rev. Lett. 65 (1990) 25
108. D.J. Hinde et al., Phys. Rev. Lett. 74 (1995) 1295
109. J.P. Lestone et al., Phys. Rev. C56 (1997) R2907
110. B.P.Ajithkumar and E.T. Subramaniam – FREEDOM (Unpublished NSC report) – 1995

### 5.1.17 Complete and Incomplete Fusion in $^{16}\text{O}+^{159}\text{Tb}$ and $^{16}\text{O}+^{169}\text{Tm}$ Systems Below 7MeV/nucleon

Manoj Kumar Sharma<sup>1</sup>, Unnati<sup>1</sup>, B. K. Sharma<sup>1</sup>, B. P. Singh<sup>1</sup>, H.D. Bhardwaj<sup>2</sup>, Sunita Gupta, Rakesh Kumar<sup>3</sup>, K.S. Golda<sup>3</sup>, and R. Prasad<sup>1</sup>

<sup>1</sup>Department of Physics, Aligarh Muslim University, Aligarh-202002

With a view of studying Complete (CF) and incomplete fusion (ICF) in heavy ion (HI) reactions, we have undertaken a program of measurement and analysis of Excitation function for a large number of reactions. During the last run we have studied  $^{16}\text{O} + ^{169}\text{Tm}$  and  $^{16}\text{O} + ^{159}\text{Tb}$  systems for the excitation function (EFs) measurements at energies below 7 MeV/nucleon. Evaporation residues for the reactions  $^{16}\text{O} + ^{159}\text{Tb}$  and  $^{16}\text{O} + ^{169}\text{Tm}$  have been identified by their characteristic  $\gamma$ -decay spectra. The analysis of the excitation functions has been done using the statistical model based computer codes ALICE-91, CASCADE and PACE2. The details of experimentally measured and theoretically calculated EFs for these reactions are given elsewhere[1]. As a representative case the experimentally measured and theoretically calculated EFs for some reactions are shown in Fig. 1.

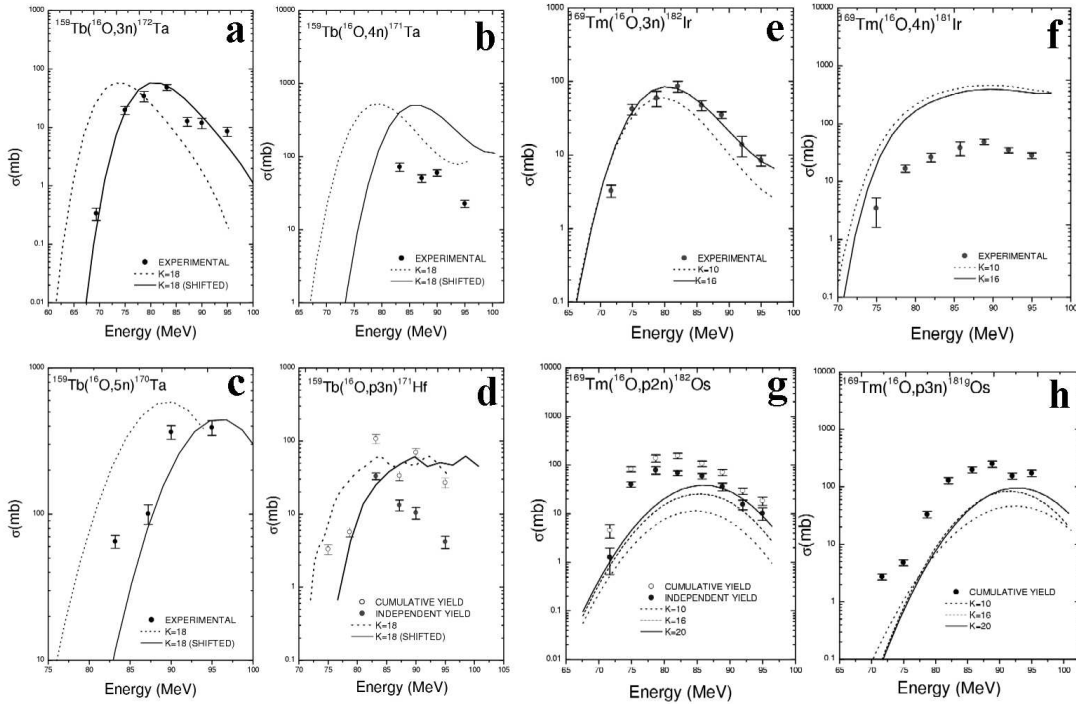


**Fig. 1 : Excitation functions for the evaporation residues in the reactions  $^{16}\text{O} + ^{159}\text{Tb}$  and  $^{16}\text{O} + ^{169}\text{Tm}$ . Dashed curves are theoretical predictions. Effect of  $E_{\text{rot}}$  on theoretical predictions are shown as solid curves**

Since in the calculations done using these codes, the ICF has not been taken into account, the enhancement of the experimental cross-sections in comparison with the theoretical predictions has been attributed to the ICF channels. Further, in order to separate out the contributions of CF and ICF, the recoil range distribution (RRD) of residues produced in the systems  $^{16}\text{O} + ^{159}\text{Tb}$  at 88 MeV and  $^{16}\text{O} + ^{169}\text{Tm}$  at 86.6 MeV have also been measured. The analysis of the RRD data has indicated

substantial contribution from the ICF of the oxygen ions. As a representative case, the RRD measurements for reaction  $^{16}\text{O} + ^{169}\text{Tm}$  at 86.6 MeV is shown in Fig. 2. As can be seen from these figures, the different peaks in the recoil range distribution occur at different cumulative thickness corresponding to the ranges of CF and ICF products.

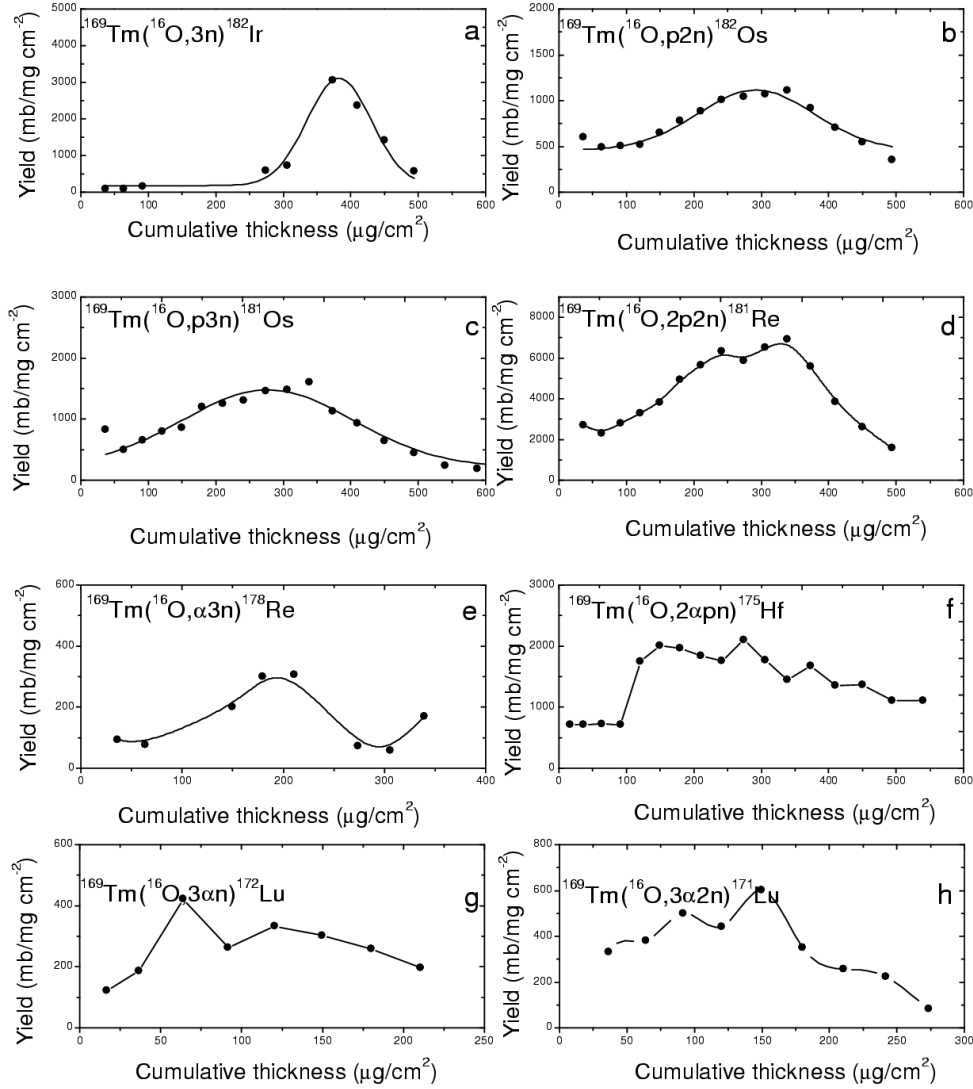


**Fig. 2 : Experimentally measured recoil range distributions for the residues produced in  $^{16}\text{O} + ^{169}\text{Tm}$  at 86.6 MeV**

## REFERENCE

111. Manoj Kumar Sharma, Ph.D. Thesis-2002, A. M. U, Aligarh.

### 5.1.18 Complete and Incomplete Fusion Reactions in $^{12}\text{C} + ^{59}\text{Co}$ via Excitation functions and Recoil Range Measurements

Avinash Agarwal<sup>1,2</sup>, I.A. Rizvi<sup>2</sup>, B.K. Yogi<sup>3</sup>, Rakesh Kumar<sup>4</sup> and A.K. Chaubey<sup>2</sup>

<sup>1</sup>Department of Physics, Bareilly College Bareilly 243 005

<sup>2</sup>Department of Physics, A. M. U. Aligarh. 202 002

<sup>3</sup>Department of Physics, Govt. College, Kota.

<sup>4</sup>Nuclear Science Centre, New Delhi – 110 067.

In recent years, considerable efforts have been devoted to the study of heavy ion (HI) induced reactions at projectile energies from the coulomb barrier to about 10 MeV/nucleons. At projectile energies closed to coulomb barrier the HI reactions are dominated by compound nucleus reactions. When the incident energy is increased the incomplete fusion (ICF) reaction starts competing with the complete fusion (CF). In incomplete fusion reactions [1,2] some part of the projectile fuses with the target and rest behaves essentially as a spectator, so that only a fraction of incident momentum is transferred, whereas complete fusion reactions involve full momentum transfer.

In the present work we have made an attempt to measure the excitation functions and recoil range distribution of the nuclides produced in the reaction using activation technique. The system under investigation was  $^{12}\text{C} + ^{59}\text{Co}$ .

For excitation function measurements, the targets of  $^{59}\text{Co}$  (thickness  $350 \mu\text{g}/\text{cm}^2$ ) were made by vacuum evaporation technique on  $2 \text{ mg}/\text{cm}^2$  aluminum foils. Individual targets were irradiated with  $^{12}\text{C}^{5+6+}$  beam at five different energies viz., 60, 65, 70, 75, and 80 MeV. Keeping in mind the half-lives of interested residues, the irradiations were performed for 10 to 12 hrs each, in GPSC facility at NSC New Delhi. The gamma activities produced in the target-catcher assembly were followed off-line using high resolution HPGe detector. The gamma ray spectrums thus obtained were analyzed using NSC developed software 'Freedom'. Excitation functions for six evaporation residues viz.,  $^{67}\text{Ge}$ ,  $^{67}\text{Ga}$ ,  $^{66}\text{Ga}$ ,  $^{65}\text{Ga}$ ,  $^{63}\text{Zn}$  and  $^{61}\text{Cu}$  have been measured. The detail of formulation used in the present investigations is reported in our earlier publication [3]. The experimental data is compared with that obtained from calculations using Alice-91 code [4]. The results indicate the presence of incomplete fusion process in the production of one alpha and two alpha emission products. As a representative case, the excitation functions of  $^{59}\text{Co}(\text{C}, 2\text{p}2\text{n})$  reaction is shown in Fig. 1.

In order to have a further confirmation to above results, the measurement of recoil range distribution of these isotopes have also been carried out at projectile energies 75 MeV and 80 MeV. Self-supporting targets of  $^{59}\text{Co}$  (thickness  $\approx 170 \mu\text{g}/\text{cm}^2$ ) backed by a stack of thin aluminum catcher foils (thickness  $\approx 75 \mu\text{g}/\text{cm}^2$  to  $100 \mu\text{g}/\text{cm}^2$ ) were used for the RRD measurements. The final stacks thus formed were irradiated at 75 and 80 MeV projectile energies for duration of about 26 hours each. The cross-sections corresponding to the various radioactive residues in each catcher were computed using

their characteristics  $\gamma$ -rays in each catcher foils. The formulation used is same as for excitation function measurements [3].

For recoil range distribution RRD measurement the cross-sections measured in each foil was divided by the respective foil thickness (in  $\text{mg}/\text{cm}^2$ ) to obtain the yield ( $\text{mb}\cdot\text{cm}^2/\text{mg}$ ), which was plotted against the cumulative catcher thickness to obtain the RRD. As a representative case the recoil range distribution of  $^{29}\text{Cu}$  residual isotope produced by  $(\text{C}, 2\alpha 2n)$  reaction is shown in Fig. 2. The size of the circle includes the errors in the experimental data. The RRD for evaporation residue peak at two values of cumulative catcher thickness, one corresponding to the complete fusion and other at lower value of range. The two peaks in the range distribution indicate that this product is also formed partly by incomplete fusion.

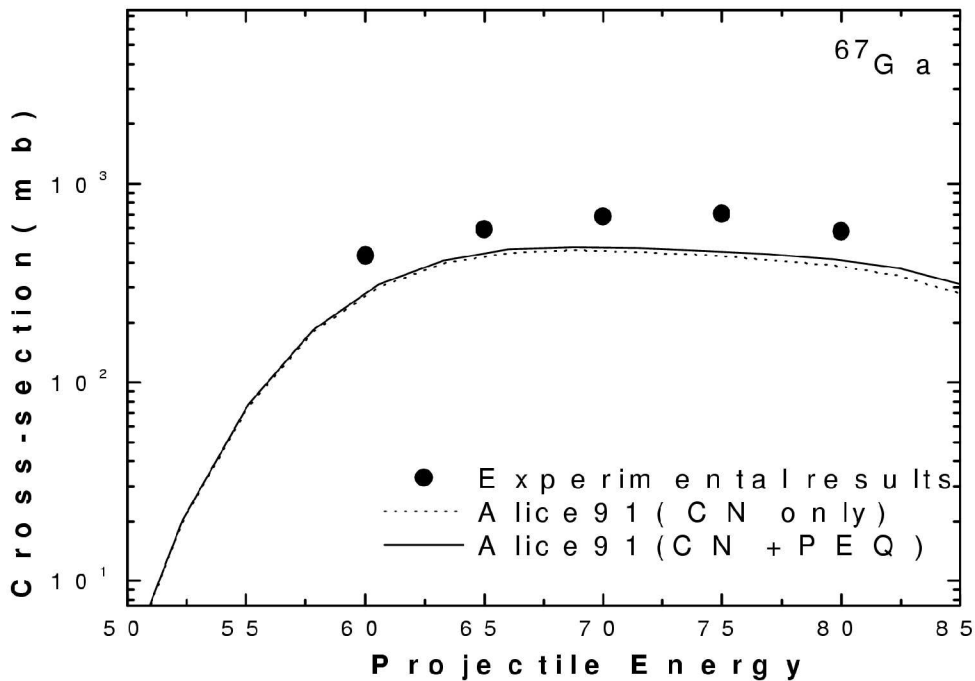
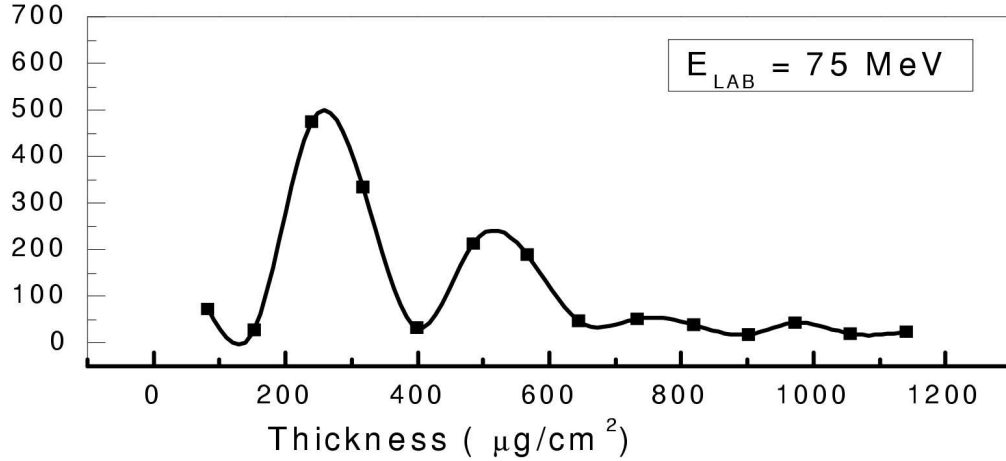


Fig. 1 : Excitation functions for  $^{59}\text{Co}(\text{C}, 2\text{p}2\text{n})^{67}\text{Ga}$

Yield ( $\text{mb}/\text{mg}\cdot\text{cm}^{-2}$ )



**Fig. 2 : Recoil range distribution of  $^{61}\text{Cu}$  at projectile energy 75 MeV**

## REFERENCES

112. C. Gerschel, Nucl. Phys. A387 (1982) 297.
113. R. H. Siemssen, Nucl. Phys. A400 (1983) 245.
114. Avinash Agarwal, I. A. Rizvi and A. K. Chaubey, Phys. Rev. C65 (2002) 34605
115. M. Blann, ALICE/91, LLNL/IAEA/NEA Data Bank France, 1991.

### 5.1.19 Measurement of the Nuclear g-Factor of $9/2^-$ and $21/2^-$ Isomeric States in $^{175}\text{Ta}$

V. Kumar<sup>1</sup>, P. Thakur<sup>1</sup>, R. Dogra<sup>1</sup>, A.K. Bhati<sup>1</sup>, S.C. Bedi<sup>1</sup>, S. Muralithar<sup>2</sup>, R.P. Singh<sup>2</sup> and R.K. Bhowmik<sup>2</sup>

<sup>1</sup>Department of Physics, Panjab University, Chandigarh - 160 014, India

<sup>2</sup> Nuclear Science Centre, New Delhi - 110 067

The present measurements are the part of systematic investigations of the static electromagnetic moments of  $9/2^-$  and  $21/2^-$  isomeric states in odd-A Ta nuclei. The lighter isotopes,  $^{171}\text{Ta}$  and  $^{173}\text{Ta}$  have been found to have decay properties different from those of heavier isotopes  $^{175-181}\text{Ta}$ , where the configuration assignments of the low-lying Nilsson proton intrinsic states have been firmly established. The  $9/2^-$  ( $E=132$  keV,  $T_{1/2}=222$  ns) and  $21/2^-$  ( $E=1565.9$  keV,  $T_{1/2}=1950$  ns) isomeric states are identified in  $^{175}\text{Ta}$  [1] nucleus as single quasiproton and three quasiparticle states, respectively.

The isomeric states in  $^{175}\text{Ta}$  have been populated through the nuclear reaction  $^{160}\text{Gd}(^{19}\text{F}, 4n\gamma)^{175}\text{Ta}$  using a 87 MeV pulsed  $^{19}\text{F}$  beam with pulse width of 2 ns and repetition period of  $1\mu\text{s}$  at 15 UD pelletron accelerator facility of Nuclear Science Centre, New Delhi. The target consisted of  $0.63$  mg/cm<sup>2</sup> enriched  $^{160}\text{Gd}$  evaporated on thick Ta backing ( $35$  mg/cm<sup>2</sup>). The external magnetic field of  $8.390(50)$  kG (measured by a Hall

probe) perpendicular to the beam-detector plane was provided by a C-type electromagnet and calibrated with respect to the magnetic moment of the  $5^{+}/2$  state ( $E=197$  keV,  $T_{1/2}=89.3$  ns) in  $^{19}\text{F}$  nucleus [2]. The perturbation of the angular distributions of the delayed  $\gamma$ -rays from the  $9/2^{-}$  and  $21/2^{-}$  isomeric states was observed in time differential mode and the extracted perturbation factors are shown in Fig. 1 and 2. From the preliminary analysis of the LSQ fitted values of the Larmor frequency  $\omega_L = g\mu_N/\hbar H$  ( $H$  is the external applied magnetic field), we obtained  $g$ -factor for  $9/2^{-}$  and  $21/2^{-}$  as  $0.644(4)$  and  $0.528(3)$  respectively. These measurements indicate the increasing trend of  $g$ -factor from  $^{171}\text{Ta}$  to  $^{175}\text{Ta}$  nuclei for the corresponding states.

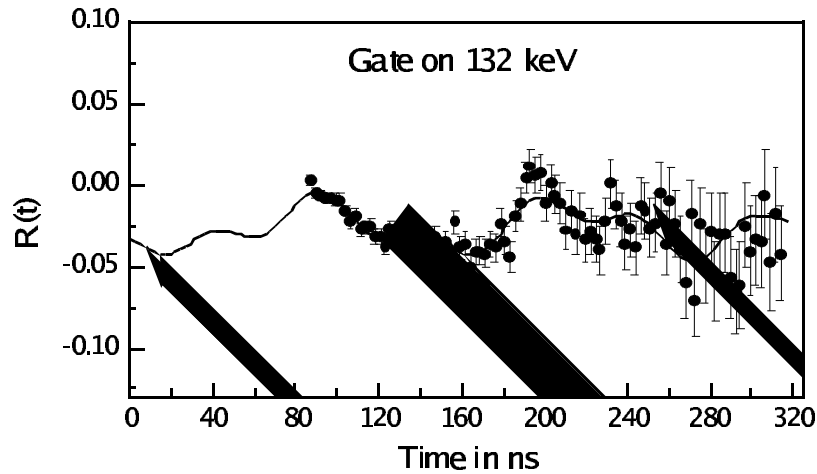


Fig. 1 : Spin rotation spectrum of  $9/2^{-}$  state in  $^{175}\text{Ta}$

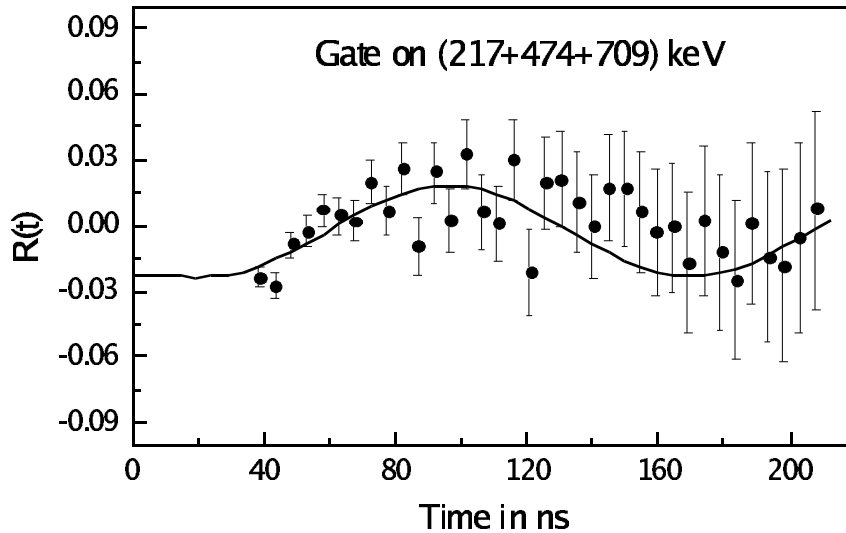


Fig. 2 : Spin rotation spectrum of  $21/2^{-}$  state in  $^{175}\text{Ta}$

## REFERENCES

116. F.G. Kondev, G.D. Dracoulis, A.P. Byrne, M. Dasgupta, T. Kibédi, G.J. Lane, Nucl. Phys. A 601 (1996) 195.
117. R. Firestone, V. Shirley, C. Baglin, C. Franck, J. Ziplin: Table of isotope, Eighth edition, John Wiley and sons inc., New York.